Escola de Camins
Escola Tècnica Superior d'Enginyeria de Camins, Canals i Ports
UPC BARCELONATECH

TREBALL FINAL DE MÀSTER

Model validation for composite structures with partial interaction

Treball realitzat per:
Joan Casas Tuneu

Dirigit per:
José Turmo Coderque
LEI Jun
XU Dong (Tongji University)

Màster en:
Enginyeria de Camins, Canals i Ports

Barcelona, juny de 2017

Departament d'Enginyeria de la Construcció

ABSTRACT

In the last decades, the use of concrete and steel composite beam structural systems has received significant attention both numerically and experimentally. This popularity is due to the advantages it provides in terms of cost, structural behaviour and construction speed. In a steel-composite beam, the compressive strength and mass of the concrete slab and the tensile strength of the steel are cleverly combined, and connected with shear struts so that they act compositely.

Depending on the grade of connection between both elements, given mainly by the type and number of shear struts, composite beams can be classified in beams with full composite action, with partial composite action or without composite action. In this latter two cases, there exist a relative slip at the interface of both materials. Traditionally, some assumptions were considered in previous studies regarding this horizontal displacement.

In this study, by means of the strength of materials theory, it is sought to validate the hypothesis which considers that the horizontal displacement at the centroid of any cross section is equal to the horizontal displacements at the cross-section edges, which has been considered in former researches. To do so, it has been applied an update on the assumption regarding the horizontal displacement at the interface of a simply supported composite beam with partial interaction being null. The slip in this case is the highest possible, therefore it is sufficient to validate composite beams with partial interaction at any rate.

This study is aimed to developed a numerical method able to solve the equations defining the stated problem and analyse whether the new assumption on the horizontal displacement may mean a significant effect for modelling composite beams with partial interaction.

ACKNOWLEDGMENTS

This master thesis has been achieved thanks to many people who have helped me during this trip full of work, passion and effort.

First of all, I would like to thank professor José Turmo, director of my thesis, for the offered help and the opportunity he gave me to work with him and to acquire more knowledge.

Secondly, I especially appreciate Lei Jun, for his dedication and enthusiasm. The provided guidance and shown passion made me take the work more powerfully.

Finally, but not less important, I would like to thank all my family, friends and acquaintances, especially my father Joan Ramon, for his passion and expertise, my mother Maria, for being my beacon of hope during tough times, my two brothers and my grandmother. Without any of them this professional and personal learning would not have been possible.

This work was partially funded by the Spanish Ministry of Economy and Competitiveness and the FEDER funds through the grant project (BIA2013-47290-R) directed by José Turmo.

CONTENTS

LIST OF FIGURES

LIST OF TABLES

1. INTRODUCTION

1.1 GENERAL ASPECTS

In the last decades, the use of concrete and steel composite beam structural systems has received significant attention both numerically and experimentally. This popularity is due to their construction speed together with structural and cost advantages. In a steel–concrete composite beam the tensile strength of the steel and the compressive strength and mass of the concrete slab are exploited. These two materials are connected with shear struts so that they act compositely. For a composite beam with rigid shear connection, there is full interaction between the steel and the concrete members. In this case, there is no relative slip at the interface of both materials and Navier hypothesis is fully applicable. This approach is followed by most codes. Nevertheless, all shear connections are flexible to some extent and therefore, full interaction is rarely achieved in practice. For this reason, partial interaction, with a relative slip at the interface, commonly appears in actual structures. The simulation of this relative slip is of primary importance because it affects both the deflections and the stresses in both the concrete and steel members. Therefore, partial interaction occurs to some extent in all beams whether fully connected or not.

By means of the theory of strength of materials, there appears a review on the definition of the slip at the interface surface and its horizontal displacement. Due to this, it is established the need to generate a new model and compare its results with the ones from the previous models.

1.2 OBJECTIVES

The main objective of this thesis is to present an efficient procedure to analyse the behaviour of composite beams with partial interaction by the means of the hypothesis of Euler-Bernoulli for Strength of Materials theory and prove the validity of previous models, compared to this new approach.

The overall aim of the work is to improve the understanding on the steel-concrete composite beams, and obtain a different approach for analysing this structural composition, compared to previous researches.

The specific objectives, aimed to achieve the main goals are:

- Study previous models used to model composite beams and compare them to the new approach presented in this thesis.
- Present a numerical model able to analyse composite beams with no interaction and run a parametric study
- Establish if the update on the hypothesis to calculate and model composite beams without full interaction may represent a needed change from previous models.

1.3 STRUCTURE OF THE THESIS

For the attainment of above objectives, the thesis is organized in six chapters, as follows:

- **Chapter 1 – Introduction**, presents the general aspects regarding this study: a short introduction, established objectives and the organization of the thesis.
- **Chapter 2 – State of the art**, introduces the present knowledge in steel-concrete composite beams as long with the theory used in the thesis to model beams.
- **Chapter 3 – Previous models and background,** presents two models, one analytical and other numerical used to model composite beams with partial interaction and the motivation for the new approach to the composite beam modelling.
- **Chapter 4 – Description of the proposed model,** describes the proposed method, presenting its equations, some numerical issues and the step-by-step description of the code.
- **Chapter 5 – Application of the proposed model,** shows different applications in realistic situations to validate the model itself and compare its results with the ones obtained from the former researches.
- **Chapter 6 – Conclusions and further investigation,** gathers the conclusion that can be extracted from the thesis and suggests some possible future lines of investigation.
- **Bibliography**

2. STATE OF THE ART

2.1 INTRODUCTION

Composite structures have represented a great progress in the construction field. The use of this structural technique in bridge and building construction is frequent and has increased considerably over the past forty years, especially due to the structural behaviour together with construction speed and material savings.

Materials usually used are concrete and steel, acting compositely. Both materials can take a roll in composite structures in different ways. On one hand, steel may be used either as a structural steel or as reinforcement bars of the concrete.

On the other hand, concrete will not only be poured concrete, but in some cases precast concrete may also be utilized. In addition, concrete can be placed either in the upper part or in the inner part of the composition.

Concrete acts at its maximum capacity under compression stresses and with minimum costs, whereas it is fragile for tensile stresses. As opposite, steel develops its highest structural capacity under tensile stresses; even stressed fibres are able to work in the plastic region.

Taking advantage of each material and their structural capacities, typical composition of a composite beam is a concrete slab supported by a steel beam. This is mainly due to their structural behaviour together with construction speed and material savings. Composite action enhances structural efficiency by combining the tensile strength of the steel and the compressive strength and mass of the concrete slab.

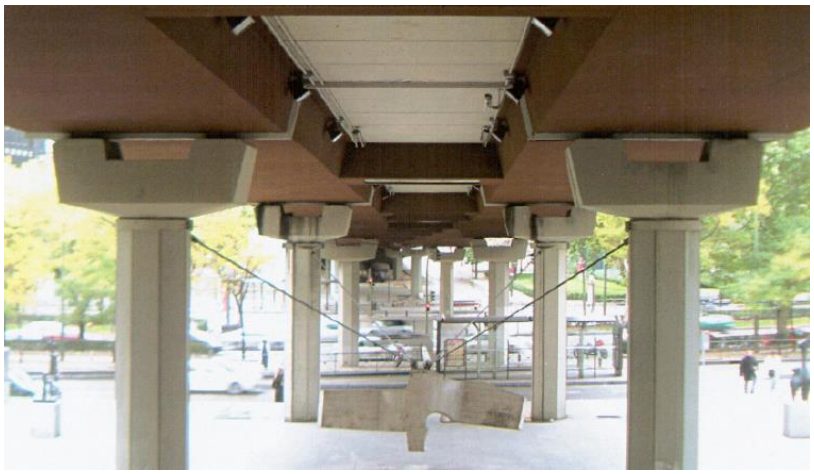

Figure 1. Juan Bravo overpass (Source: Puentes Estructuras Actitudes)

The key to take advantage of both materials is that they both must act compositely. In order to do so, both materials are connected with shear connectors. For a composite beam with rigid shear connection, there is full interaction between the steel and the concrete members. Therefore, in this case, there is no relative slip at the surface of contact of both materials and Navier-Bernoulli hypothesis are fully applicable. Nevertheless, all shear connections are flexible to some extent; hence, full interaction is rarely achieved in practice. For this reason, partial interaction with a relative slip at the interface commonly appears in actual structures. Using partial connection gives the opportunity to achieve a better match between applied and resisting moment and even some economy in the provision of connectors.

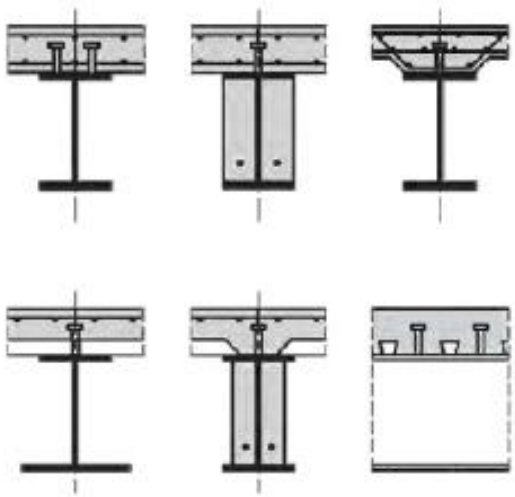

Figure 2. Typical cross sections of composite beam (Source: Docotal thesis by B. Gil Rodríguez)

The simulation of this relative slip is of primary importance because it affects both the deflections and the stresses in the concrete slab and the steel frame.

The distinction between steel-concrete composite beams with full and partial interaction, and without interconnection is shown in Figs. 3 to 5. For partial action, it can be noticed that the relative slip is relatively large, whereas in the case of fully composite beam the slip is really small.

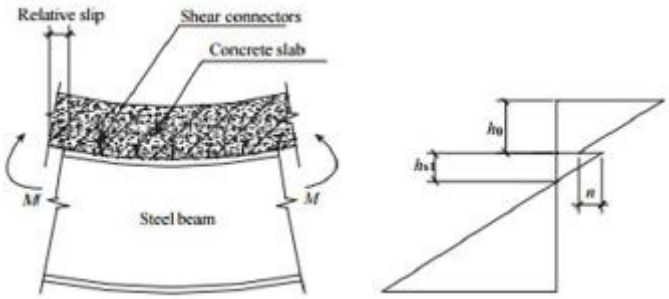

Figure 3. Beam with partial composite action: (left) force and deformation of steel beam and concrete slab; (right) stress distribution along section height (Li et al. 2007)

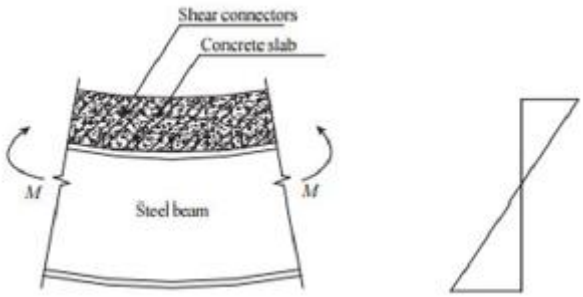

Figure 4. Beam with full composite action: (left) force and deformation of steel beam and concrete slab; (right) stress distribution along section height (Li et al. 2007)

Finally, for a beam without composite action at all, both materials act individually and are both under tensile and compression stresses.

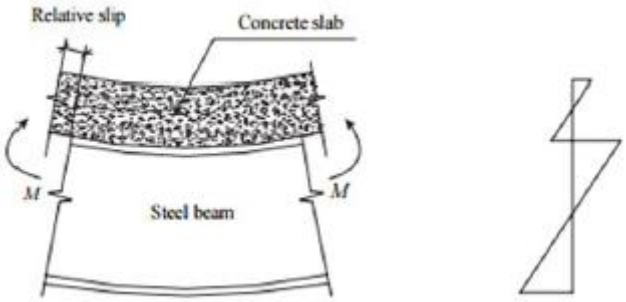

Figure 5. Beam without composite action: (left) force and deformation of steel beam and concrete slab; (right) stress distribution along section height (Li et al. 2007)

According to EN-1994-1-1 2004, which is the Eurocode norm for designing composite steel and concrete structures, a composite beam shall be checked for: resistance to longitudinal shear, resistance of critical cross sections, resistance to lateral-torsional buckling, resistance to shear buckling and transverse forces on webs.

The bending resistance of the composite cross section highly depends on the effective width of the concrete slab, which represents the width of the portion of a concrete slab considered effective in resisting compression, at a composite beam cross section. This width is different in hogging and sagging bending moment regions, as well as in elastic and plastic phase. For elastic analysis, this effective width problem is simplified by assuming a constant effective width over the whole of each span.

There exist different types of shear connectors between the two components, presented in Figs. 6 to 8. The most widely used type of connector is the headed stud shear connector (Fig. 7).

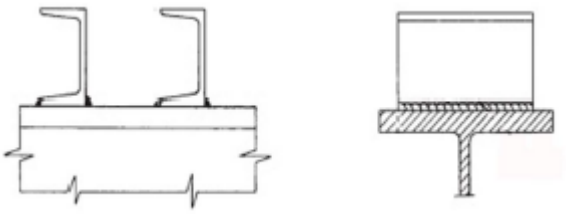

Figure 6. Channel connectors (Johnson 2004)

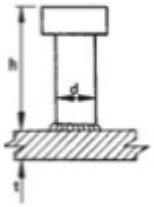

Figure 7. Headed stud (Johnson 2004)

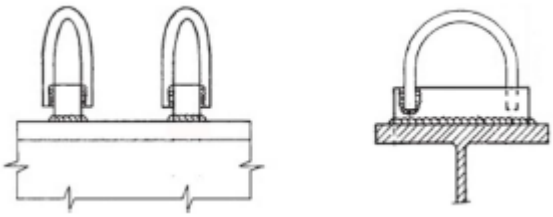

Figure 8. Bar connectors (Johnson 2004)

This shear connectors must be designed to prevent separation and uplift between the concrete slab and the steel frame.

2.2 EULER-BERNOULLI BEAM THEORY

For the present thesis, the Euler-Bernoulli hypothesis are considered. It is based on the elastic theory and assumes that cross section is perpendicular to the centroid along the whole beam when it is bent under vertical loads. These assumptions work better for beams with large relations between length and thickness.

3. PREVIOUS MODELS AND BACKGROUND

3.1 INTRODUCTION

Some studies have focused on finding the behaviour of composite beams, either for partial or full interaction. One of the firsts works to do so, was the one conducted by *J. Martínez Calzón,* gathered in the book titled "Construcción mixta. Hormigón-Acero". Ever since, some other researches have been developed, taking advantage of the advance in computing facilities, such as finite element method. This method was the one used by Turmo et. al, and proposed in the paper "Modelling composite beams with partial interaction". These both methods will be presented for further comparison with the model designed in this thesis.

3.2 MARTÍNEZ AND ORTIZ

In their work, it was studied composite constant depth simply supported beams with partial interaction under simple load cases with analytical equations (Eqs. (1)-(4)). In this procedure, the equilibrium equations of the composite beam are reduced to second order differential equations from which analytical results can be obtained. These equations obtain for concrete slab axial forces at cross section x, $N_c(x)$.

The different load cases studies were: (1) a concentrated load Q applied at mid-span, (2) a constant distributed vertical q applied throughout the beam, (3) a concentrated external bending moment M_{ext} applied at one beam edge and (4) a concentrated prestressing load P is introduced at both beam edges and applied at the centroid of the concrete slab.

The different axial forces at some cross section of the beam for each load case are presented following:

$$N_{c,Q}(x) = \frac{-M(x)}{a_{cr}} \cdot \psi_Q = \frac{-M(x)}{a_{cr}} \cdot \left(1 - \frac{ch\left(\frac{l}{2 \cdot x_q}\right) - ch\left(\frac{l}{2 \cdot x_q} - \frac{x}{x_q}\right)}{\frac{x}{x_q} \cdot \frac{(l-x)}{x_q} \cdot ch\left(\frac{l}{2 \cdot x_q}\right)} \right) \qquad (1)$$

$$N_{c,q}(x) = \frac{-M(x)}{a_{cr}} \cdot \psi_q = \frac{-M(x)}{a_{cr}} \cdot \left(1 - \frac{x}{x_q} \cdot \frac{sh\left(\frac{x}{x_q}\right)}{ch\left(\frac{l}{x_q}\right)} \right) \tag{2}$$

$$N_{c,M}(x) = \frac{-M_{ext} \cdot x}{L \cdot a_{cr}} \cdot \psi_M = \frac{-M_{ext} \cdot x}{L \cdot a_{cr}} \cdot \left(1 - \frac{sh\left(\frac{x}{x_q}\right)}{\frac{x}{l} \cdot sh\left(\frac{l}{x_q}\right)} \right) \tag{3}$$

$$N_{c,P}(x) = -\zeta_c \cdot P - \zeta_S \cdot P \cdot \varepsilon_S =$$
$$= -\left(1 + \frac{A_s^2 \cdot h_{sc}^2}{A_R \cdot I_R}\right) \cdot \frac{A_{cR} \cdot P}{A_R} - \left(1 - \left(1 + \frac{A_s^2 \cdot h_{sc}^2}{A_R \cdot I_R}\right) \cdot \frac{A_{cR}}{A_R}\right) \cdot P \cdot \frac{ch\left(\frac{x}{x_q} - \frac{l}{2 \cdot x_q}\right)}{ch\left(\frac{l}{2 \cdot x_q}\right)} \tag{4}$$

As an additional and needed information:

$$a_{cr} = \frac{I_R \cdot A_R}{h_{sc} \cdot A_{cR} \cdot A_S} \tag{5}$$

$$x_q = \sqrt{\frac{(I_S + I_{cR}) \cdot s_q \cdot E_S}{a_{cr} \cdot h_{sc} \cdot n_q \cdot k_q}} \tag{6}$$

In these equations:

- $M(x)$ is the bending moment at cross section x
- E_C and E_S are the Young's Modulus in concrete slab and steel beam respectively.
- A_R and I_R are the area and inertia of the reduced composite section
- A_{cR} and I_{cR} are the reduced area and inertia of the concrete section
- A_S and I_S are the area and inertia of the steel section
- h_{sc} is the distance between the concrete slab centroid and the steel beam centroid
- k_q is the connector stiffness under shear force
- s_q js the shear connector longitudinal spacing
- n_q is the number of shear struts in every row separated s_q

In Fig.9 is shown a scheme of the different parameters which define the model.

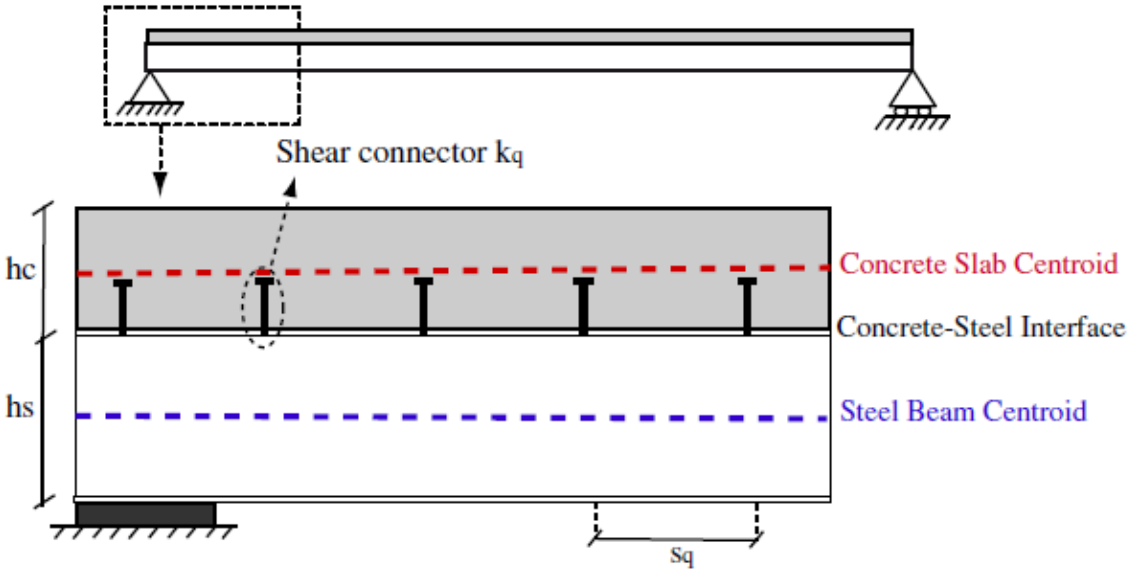

Figure 9. Composite beam and parameters of the model (J. Turmo et al. 2015)

These equations are based on the following assumptions:

- Concrete slab and steel beam have the same curvature (and same rotation) throughout the length of the composite beam.
- Shear connectors, as well as concrete and steel, behave linearly.
- The discrete shear connectors at the concrete-steel interface are uniform throughout the length of the composite beam.
- Frictional effects and uplift at the concrete-steel interface are neglected.

In addition to their computational cost, the limitation of the analytical equations refers to their application restrictions. Actually, these equations cannot be applied in a number of practical design solutions (such as tapered beams, non-continuous shear connector distributions or complex load cases). For continuous beams, support reactions are unknown. For this reason, these structures cannot be analysed with those formulas unless it is assumed that the reactions of a continuous beam are not affected by the partial interaction.

3.3 MODELLING COMPOSITE BEAMS WITH PARTIAL INTERACTION

The paper *Modelling composite beams with partial interaction,* by Turmo et al., focused on create a finite element model for the analysis of composite beams with partial interaction. To validate the accuracy of the proposed model, a set of FEMs were verified against those results obtained by analytical equations present in the literature, such as J. Martínez and J. Ortiz, for different loading and boundary conditions.

The advantages of this model compared with the literature are as follows:

- Applicability, as the method provides useful information for the design in practical work.

- Possible widespread use of the model, as it can be implemented in any structural software.
- Versatility in dealing with any combination of loading and boundary conditions.
- Intuitiveness, as the different elements of the model present an easy and close to understand relation with the structural behaviour of the composite beam.
- Easy elaboration of models.

The elements of the model are uniquely beam elements. The different elements of the composite beams are modelled by six different types of frame elements (concrete slab, steel beam, vertical struts, spring shear connector elements and elements representing concrete thickness and steel thickness). It uses same parameters and layout shown in Fig. 9.

3.4 MOTIVATION FOR THE PROPOSED MODEL

Both previously presented models assume that concrete slab and steel beam have the same curvature, which means that both centroids have the same curvature. This condition may also be achieved by the means of the theory of strength of materials, which is stated following.

In a general overview, a concrete slab fully supported on a steel beam, with no connection between both at all, subjected to an arbitrary load p(x), perpendicular to the contact surface between beams and applied on the upper beam. (Fig 10 (up)). After bending, the shape of the structure is shown in Fig. 10 (down).

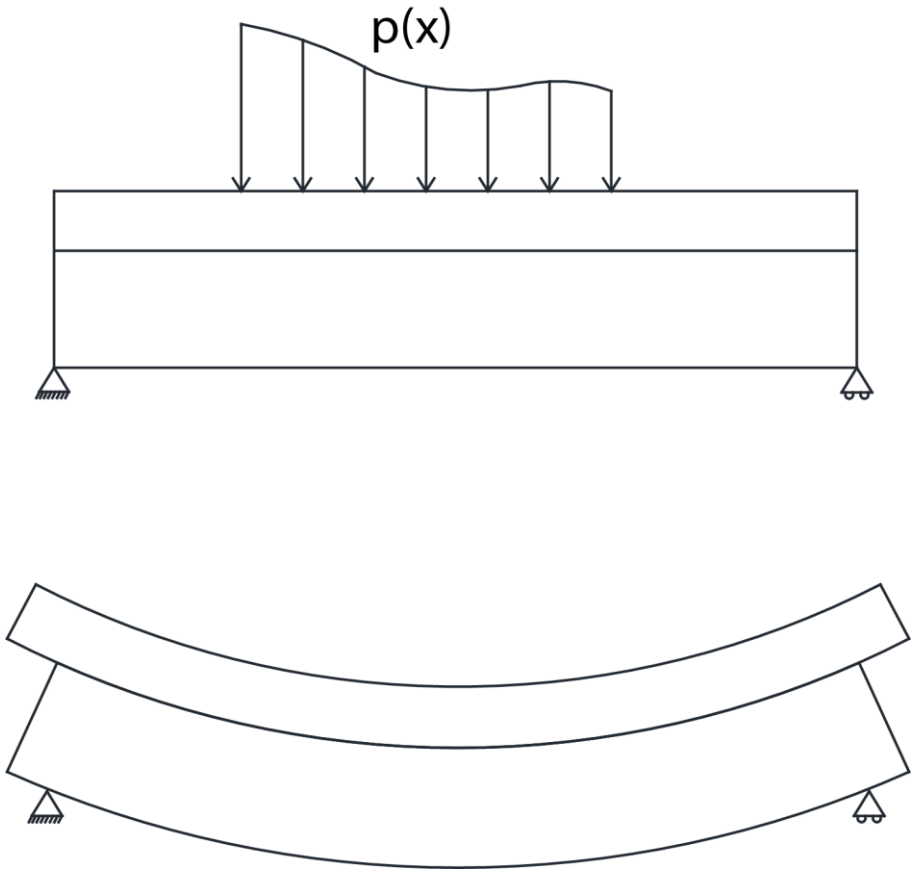

Figure 10. (Up) Composite beam under load p(x). (Under) Estimated deformed shape of the composite beam due to load p(x)

In this situation, there exists free slip between both members, hence there is no shear stress along the contact surface and friction may be neglected.

Regarding the stress analysis of the system, which is static determinate beam for the boundary conditions, but static indeterminate internally, it seems logic that compatibility equations assure no uplift between both beams, or in other words, that both beams present same deflections. This fact is stated in equation (7):

$$\theta_{oc} X_c + \int_0^X \kappa_c(x) \cdot (X - x)\, dx = \theta_{os}\, X_s + \int_0^X \kappa_s(x) \cdot (X - x)\, dx \tag{7}$$

Where, rotations are given by the integration of curvatures as:

$$\theta_{oc} = \frac{\int_0^L \kappa_c(x) \cdot (L - x)\, dx}{L} \tag{8}$$

$$\theta_{os} = \frac{\int_0^L \kappa_s(x) \cdot (L - x)\, dx}{L} \tag{9}$$

In addition, structural equilibrium must exist for each section of the beam. Therefore, having a generic load p(x), a bending moment law $M_f(x)$ and shear law $Q(x)$ are obtained.

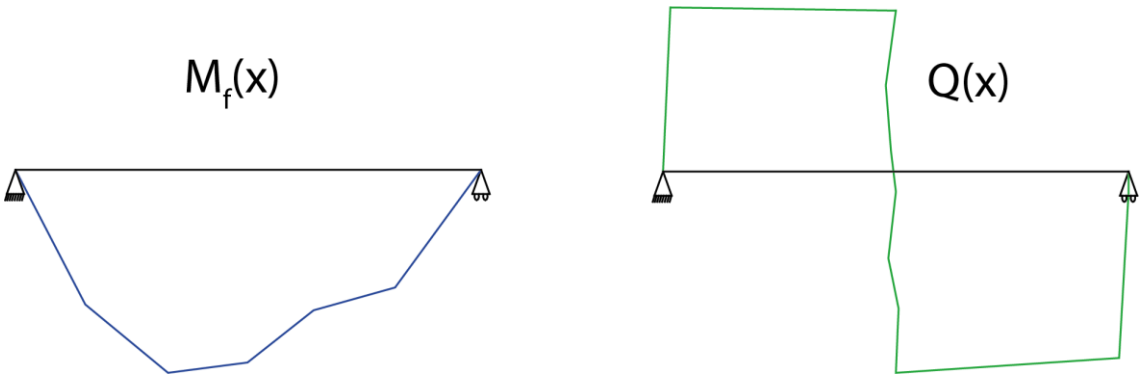

Figure 11. (Left) Bending moment law. (Right) Shear stress law

At any cross section, it will have to be fulfilled that:

$$M_f(x) = M_{f,c}(x) + M_{f,s}(x) \tag{10}$$

Developing expression in Eq.(10):

$$M_f(x) = \mathrm{E}_c I_c \kappa_c(x) + \mathrm{E}_s I_s \kappa_s(x) \tag{11}$$

Solving the differential equation, Eq. (7), it can be obtained:

$$\kappa_c(x) = \kappa_s(x) = \kappa(x) \tag{12}$$

Thus, it has been found the equality of curvature by using the theory of strength of materials. Next, expressions are further developed. By putting up together Eqs. (11) and (12):

$$M_f(x) = \kappa(x) \cdot (\mathrm{E}_c I_c + \mathrm{E}_s I_s) \tag{13}$$

$$\kappa(x) = \frac{M_f(x)}{(\mathrm{E}_c I_c + \mathrm{E}_s I_s)} \tag{14}$$

$$M_{f,c}(x) = \mathrm{E}_c I_c \frac{M_f(x)}{(\mathrm{E}_c I_c + \mathrm{E}_s I_s)} = \phi_c M_f(x) \tag{15}$$

$$M_{f,s}(x) = \mathrm{E}_s I_s \frac{M_f(x)}{(\mathrm{E}_c I_c + \mathrm{E}_s I_s)} = \phi_s M_f(x) \tag{16}$$

Therefore, the curvature law is related to the bending moment $M_f(x)$, and each beam is affected by some stress on lineal dependency with its stiffness, shown in Fig. 12. Bending moment on concrete slab ($M_{f,c}(x)$) added up to bending moment on steel beam ($M_{f,s}(x)$) equals to the total bending moment suffered by the total system. It is similar in the case of the shear stress $\mathrm{Q}(x)$.

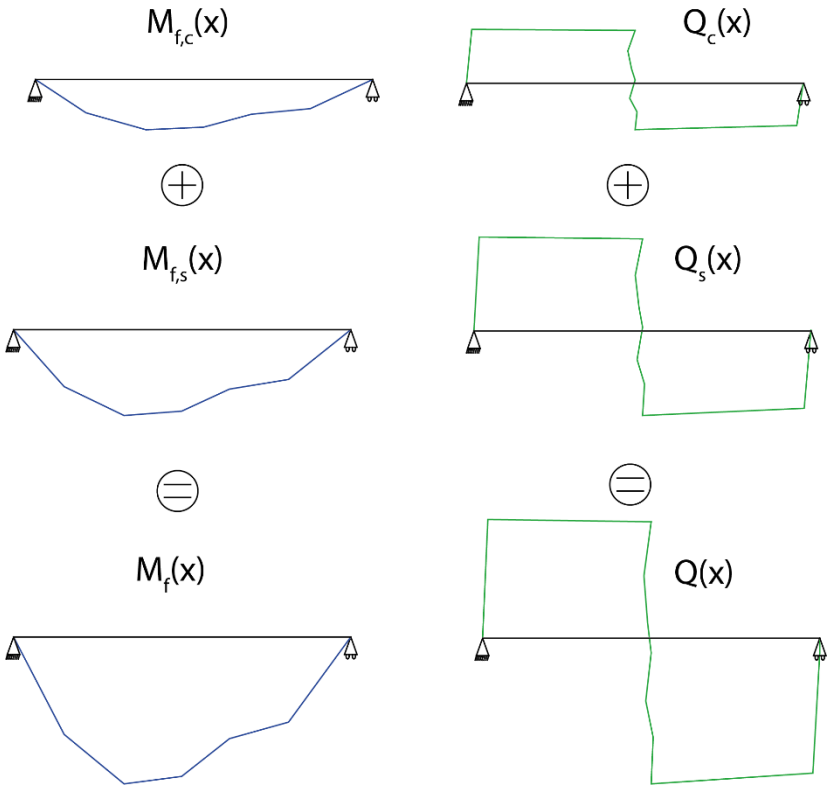

Figure 12. Bending moment law (blue) and shear stress (green)

As the load is applied directly on the concrete slab, a portion of that load, named $p_s(x)$, is not beared by the concrete and it is transferred to the steel beam at the points of application of load p(x), as well as two puntual loads $R_{1,C}$ and $R_{2,C}$, not having any other loads at any other point of the interface.

$$R_{1,C} = \frac{\mathrm{E}_c I_c}{\mathrm{E}_c I_c + \mathrm{E}_s I_s} \cdot R_1 \tag{17}$$

$$R_{2,C} = \frac{\mathrm{E}_c I_c}{\mathrm{E}_c I_c + \mathrm{E}_s I_s} \cdot R_2 \tag{18}$$

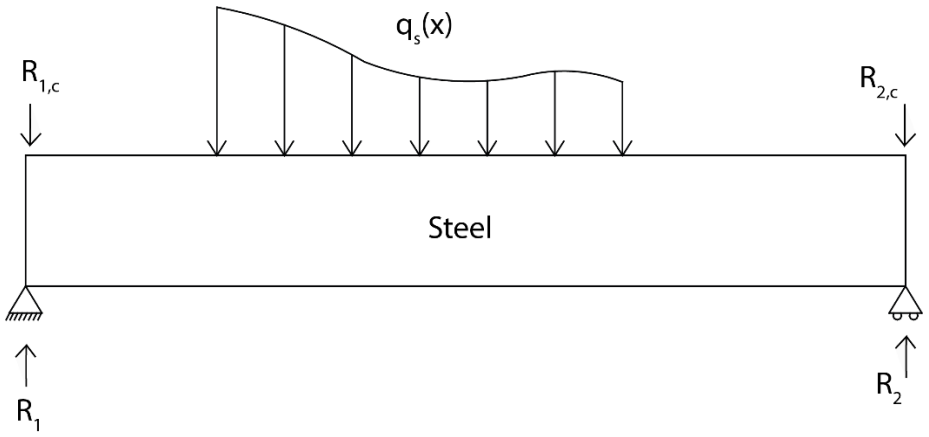

Figure 13. Transferred load to the steel beam

This, from the point of view of the load transfer, it does not make sense, as, for example, in the case with a punctual load P at mid-span, it will mean that the stress transfer will be discrete and only take place at three points of the structure, which it is not the case, as the load is transferred gradually.

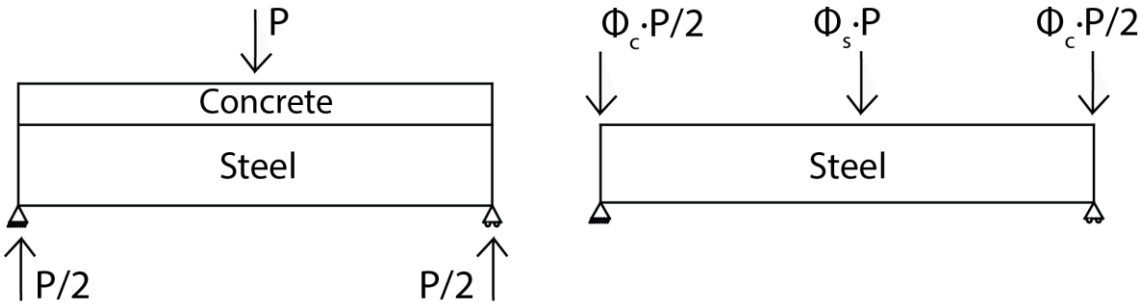

Figure 14. (Left) Punctual load at mid-span. (Right) Transferred load to the steel beam

At this point, geometry of the problem is checked. Navier-Bernoulli's hypothesis establishes that for a beam bending under vertical loads in the direction of gravity, the upper face of the beam will have a more curved shape than the centroid, and the inner face will have a less curved shape than the centroid. In Fig. 15 it can be seen that radius of the upper face, ρ_u, is smaller than the radius of the centroid, ρ_c. At the same time, this latter radius is smaller than the radius of the inner face, ρ_i. As it is known, curvature, is defined as the inverse of the radius:

$$\kappa = \frac{1}{\rho} \tag{19}$$

Therefore, each part of the beam will present different curvatures, verifying that:

$$\rho_u < \rho_c < \rho_i \tag{20}$$

$$\kappa_u > \kappa_c > \kappa_i \tag{21}$$

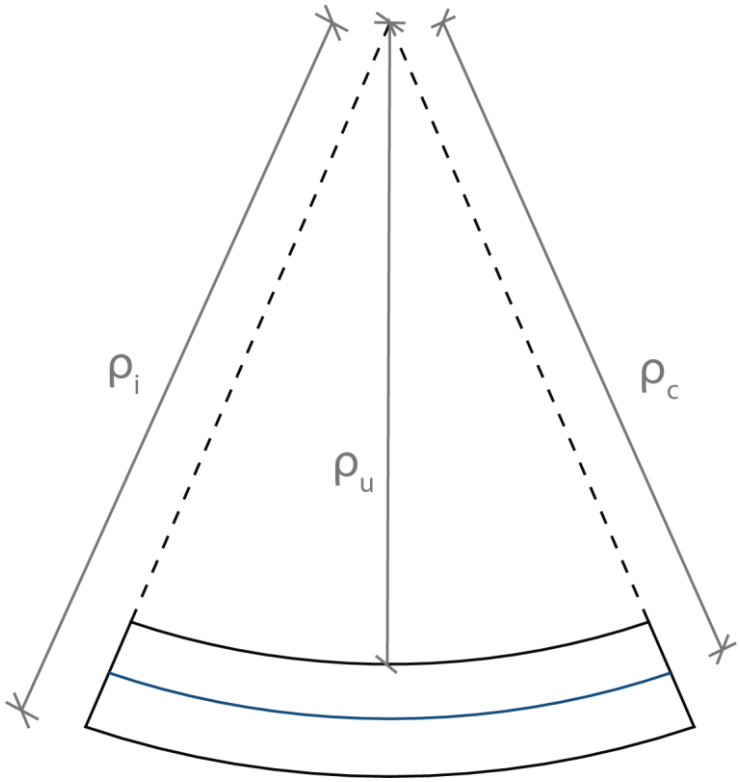

Figure 15. Radius of curvature of a deformed piece of beam. Blue line represents the centroid

Taking this into account, when placing two beams with the exact curvature of their respective centroids, the inner face of the upper beam and the upper face of the inner beam do not stay in contact along the whole length. This aspect fails the fact that both elements in a composite beam must be in contact along the total length of the beam and no uplift must appear.

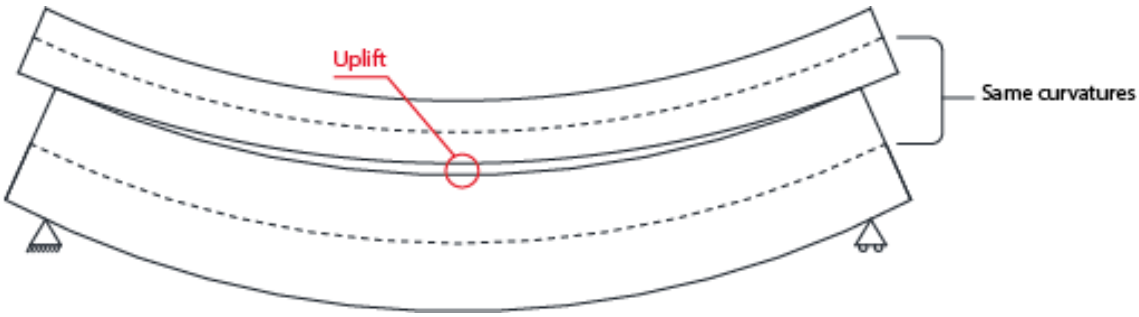

Figure 16. Layout of two superimposed beams, which their centroids have the same curvature

This situation highlights the need for a review on the application of the Strength of Materials' hypothesis, as these hypotheses are not verified in this case, and the seek for the condition that guarantees contact along the whole beam, while fulfilling Navier-Bernoulli's hypothesis.

In general terms, when finding a deflection by the theory of Strength of Materials, it is assumed that all fibers of the same cross section have the exact same vertical deflection, as rotation θ is really small. This is shown in Figs. 17-18 and stated in Eqs. (22)-(24).

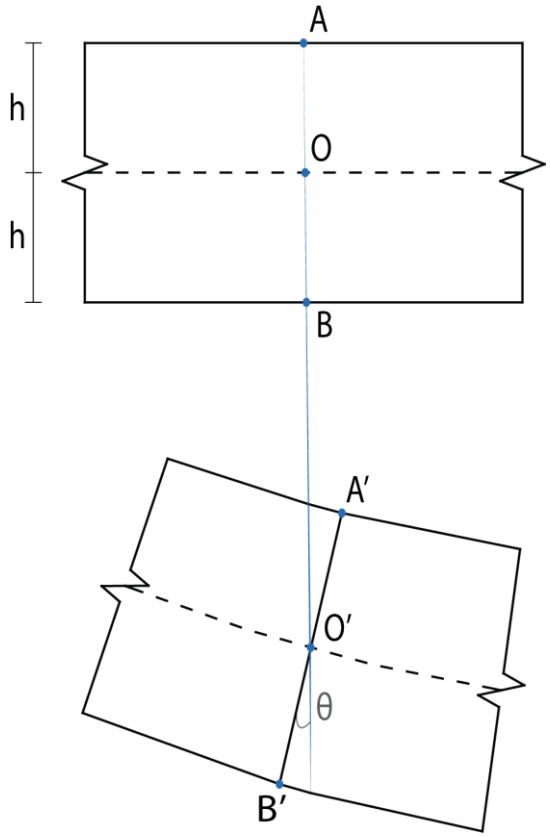

Figure 17. (Up) Detail of a non-deformed beam. (Down) Detail of a deformed beam

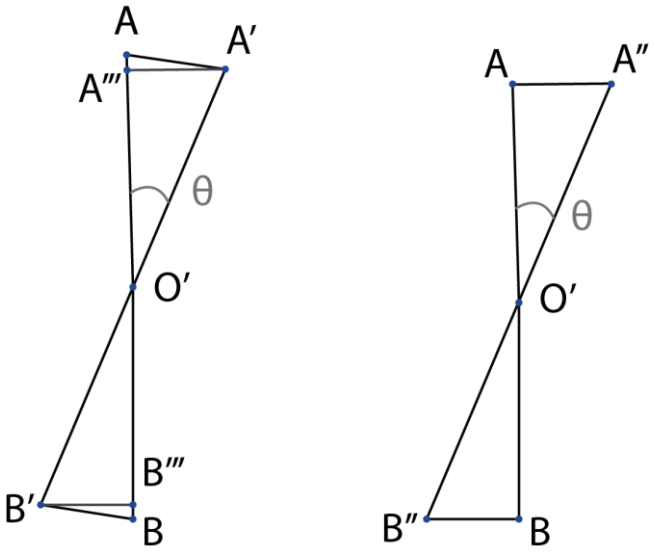

Figure 18. (Left) Detail of deflection. (Right) Assumption made by strength of materials

Deflection of point A and B can be written:

$$f_A = OO' + AO - O'A''' = f_o + h - h \cdot cos\theta > f_O \tag{22}$$

$$f_B = OO' - BO + O'B''' = f_o - h + h \cdot cos\theta < f_O \tag{23}$$

Considering θ small, cosθ can be approximated to 1:

$$f_A = f_O + h - h \cdot cos\theta \approx f_O + h - h = f_O \tag{24}$$

By Eq. (24), point A and point O are proved to have the same vertical deflection. However, they do not have the same horizontal displacement.

$$f_{h,A} = A'A''' = h \cdot sin\theta \approx h \cdot \theta = AA'' \tag{25}$$

$$f_{h,B} = B'B''' = -h \cdot sin\theta \approx -h \cdot \theta = BB'' \tag{26}$$

Where we approximate sinθ by θ.

In previous models, such as in Martínez. J (1975) and Turmo, et al. (2015), it was assumed, regarding displacements, that, for a certain coordinate, both centroids presented the same vertical and horizontal displacements alongside the cross section, before and after bending, and both centroid curvatures are considered equal.

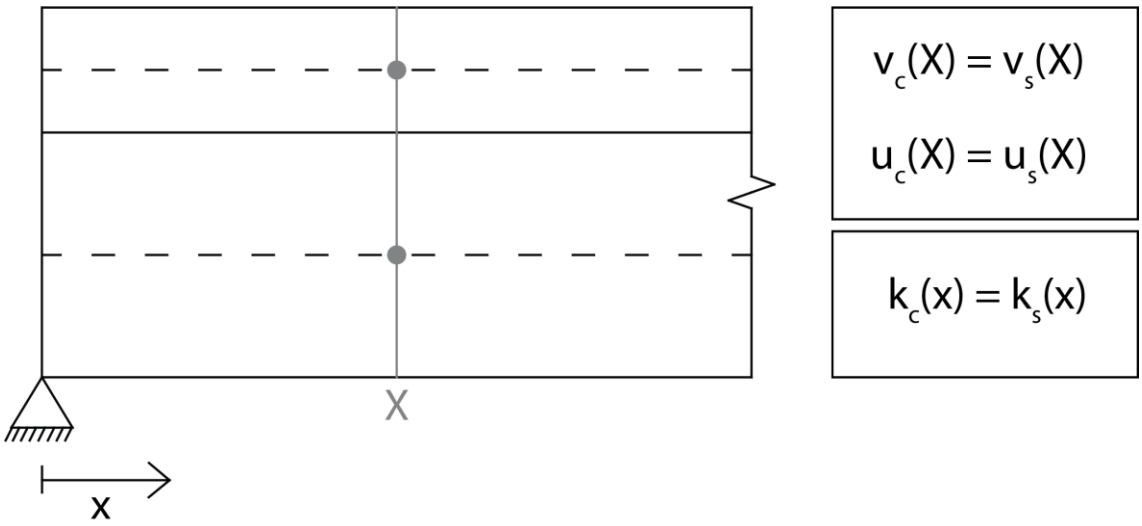

Figure 19. Vertical and horizontal displacements of both centroids considered in former researches

It has been stated previously that by means of the strength of materials, in order to keep contact between both elements along the whole beam, curvatures shall be different. Also, the horizontal displacement of two points in the same cross section is different. However, there will exist a different cross section with the same horizontal displacement after bending (Fig. 20).

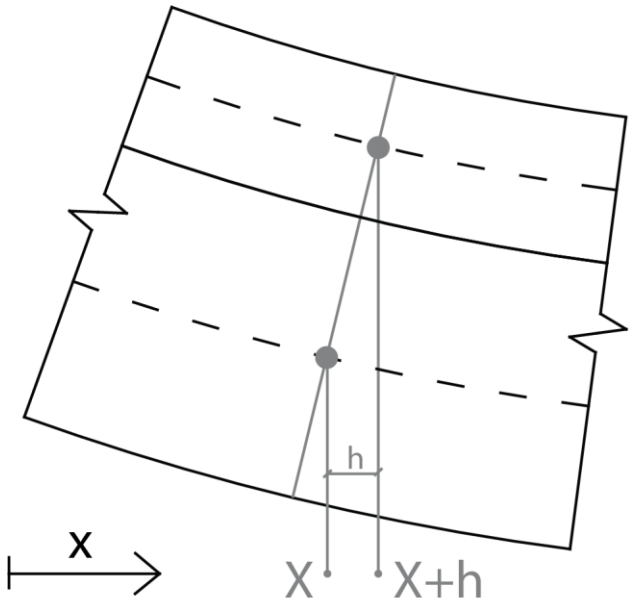

$$v_c(X) = v_s(X)$$

$$u_c(X+h) = u_s(X)$$

Figure 20. Assumption on the vertical and horizontal displacement considered in the present thesis

In the present thesis, this effect is taken into account, to finally understand if there is need of considering this effect, or it can be neglected and use the hypothesis regarding the horizontal displacement assumed so far.

It is important to highlight that, in order to verify rightfully the theory of strength of materials and to have plenty of contact along the whole length of the interface, it has been proved that both elements will have different curvatures.

4. DESCRIPTION OF THE PROPOSED MODEL

4.1 INTRODUCTION

Overall, the problem consists on finding two functions $\kappa_c(x)$ and $\kappa_s(x)$, such for all $X_S \in$ (0,L) it exists one and only one X_c, in which compatibility conditions of deflections and internal equilibrium are verified. L is the length of the beam under study.

4.2 SYSTEM OF DIFFERENTIAL EQUATIONS

There exist a system of differential equations which define

The condition for equals deflections of the upper face of the steel beam and the lower face of the concrete beam is written:

$$\begin{aligned}\theta_{oc}X_c + \int_0^{X_C} \kappa_c(x)\cdot(X_c - x)\,dx - h_c\cdot(1-\cos(\theta_{oc} + \int_0^{X_C}\kappa_c(x)\,dx)) = \\ = \theta_{os}X_s + \int_0^{X_S}\kappa_s(x)\cdot(X_s - x)\,dx + h_s\cdot(1-\cos(\theta_{os} + \int_0^{X_S}\kappa_s(x)\,dx))\end{aligned} \tag{27}$$

Where cosine of rotations is equal to 1, thus the expression can be rewritten as:

$$\theta_{oc}X_c + \int_0^{X_C}\kappa_c(x)\cdot(X_c - x)\,dx = \theta_{os}X_s + \int_0^{X_S}\kappa_s(x)\cdot(X_s - x)\,dx \tag{28}$$

Which is equal to Eq. (7).

Furthermore, the equality of horizontal coordinates for the vertical deflection states:

$$X_c + h_c\cdot\sin(\theta_{oc} + \int_0^{X_C}\kappa_c(x)\,dx) = X_s - h_s\cdot\sin(\theta_{os} + \int_0^{X_S}\kappa_s(x)\,dx) \tag{29}$$

And applying again, $\sin\theta = \theta$:

$$X_c + h_c\cdot(\theta_{oc} + \int_0^{X_C}\kappa_c(x)\,dx) = X_s + h_s\cdot(\theta_{os} - \int_0^{X_S}\kappa_s(x)\,dx) \tag{30}$$

Previous equations state the vertical deflections and the horizontal displacement conditions. Also, equilibrium conditions shall be also fulfilled. Regarding this:

$$M_f(x) = M_c(x) + M_s(x) = \kappa_c(x) \cdot \mathrm{E}_c I_c + \kappa_s(x) \cdot \mathrm{E}_s I_s \quad (31)$$

Summing up, the solution to the proposed problem, when taking into account Strength of Materials theory, is found by solving the system of non-linear equations defined by Eqs. (28), (30) and (31), with the respective boundary conditions.

4.3 NUMERICAL RESOLUTION

4.3.1 Introduction

The model will be created by using the *MATLAB software*. MATLAB stands for Matrix Laboratory and is a multi-paradigm numerical computing environment and programming language, intended primarily for numerical computing.

Some analytical and numerical arrangements have been applied to the equations established (Eqs. (29)-(31)) on the previous section, in order to obtain useful expressions of the equations that can be used for the model.

The main unknown variables are the longitudinal location of both neutral axis along the beam: X_c for the concrete and X_s for the steel; and the curvature of both elements at certain cross sections: $\kappa_c(X_c)$ for the curvature of the concrete and $\kappa_s(X_s)$ for the curvature of the steel. Furthermore, rotations for concrete and steel at one edge of the composite beam, θ_c^1 and θ_s^1 respectively, will be also unknowns. Theoretically, the number of unknowns adds up to 3N+5, where N is the number of elements in which the beam is divided. However, depending on the case of study, the number of unknowns will be less, as some of them can be considered known.

It is important to remark that on the variables; the sub index stands for the material: “s” for steel and “c” for concrete; on the other hand, the super index shows the related cross section.

As it has been previously stated, it is necessary for the process to divide the beam in equally length elements, which define the cross sections of the beam where the values of variables are calculated. These parts have their position well defined along the whole beam. In the proposed model, the beam is divided into different number of elements and it defines the position of the neutral axis of the steel, X_s. Therefore, this variable is established at the beginning of the process. The number of cross sections is N+1. Each of them is described by the letter i. Therefore, the rank of cross sections goes from i=1 to i= N+1, and i is a natural number.

The reason of choosing the location of the steel neutral axis instead of the concrete axis is due to the shape of bending of the beam under the proposed loads. Concrete slab is expected to slip over the steel beam. As shown in Fig. 21, both edges of the concrete slab will protrude over edges of the steel beam. These protruded parts of concrete fall out of the region of study as there is not contact face and equations are no validated.

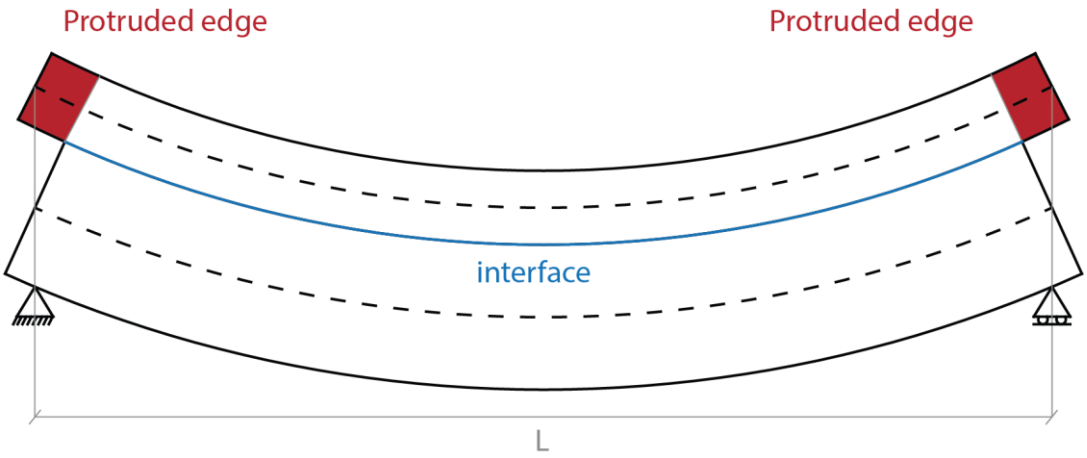

Figure 21. Interface (blue) and protruded edges (red) after bending

Steel centroid longitudinal coordinates are defined from 0 up to L. Concrete centroid longitudinal coordinates will be, hence, within these limits. (Fig. 22).

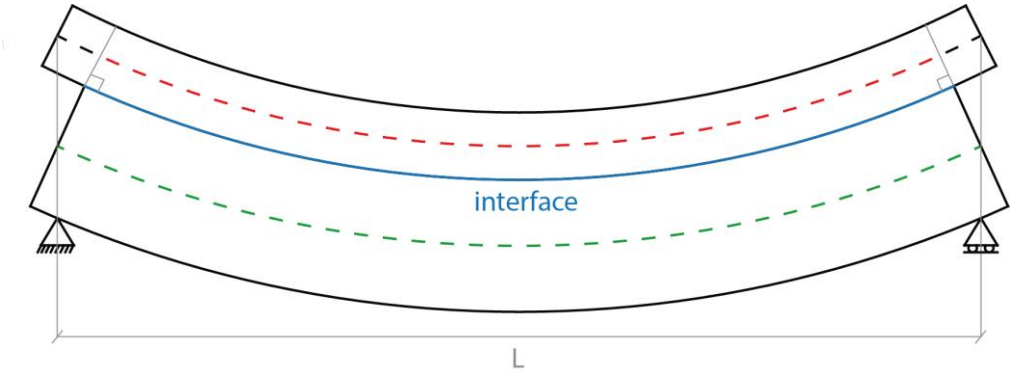

Figure 22. Steel centroid coordinates (green) and concrete centroid coordinates (red) fulfilling the equations of the model

4.3.2 Equations and unknowns

The problem to be solved is resumed in a non-linear system of equations. In order to be able to find a solution, the total number of equations must coincide with the number of unknown variables.

The number of equations and the number of unknowns depends on how many elements is divided the beam. Equations (Eqs. (32)-(34)) relates unknowns with the previous cross section and also the next one, regarding their position alongside the beam centroids.

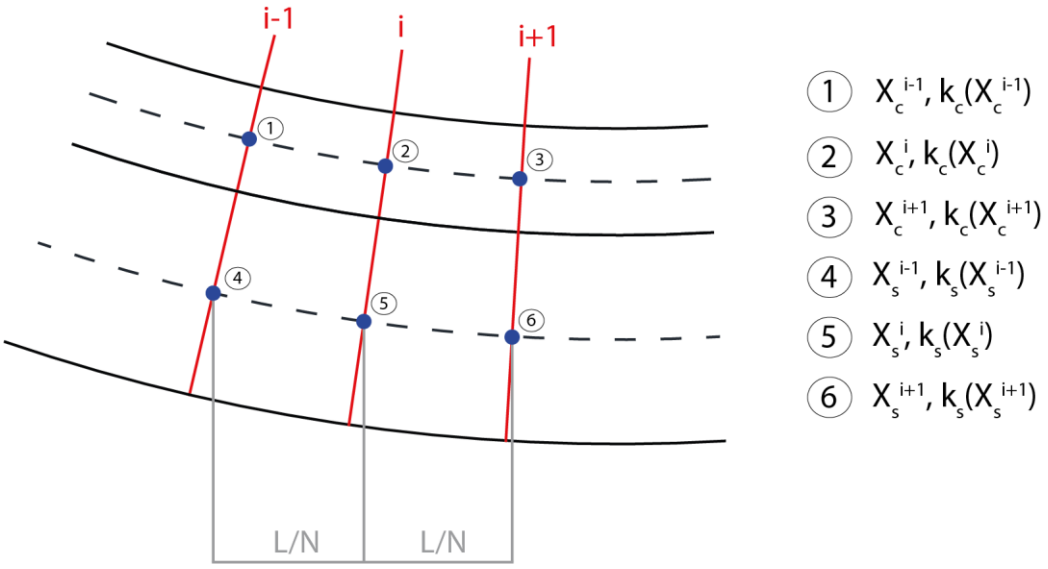

Figure 23. Variables at i-1th cross section, ith cross section and i+1th cross section

In addition, some theoretically unknown variables can be considered as known. For instance, in the case of a simply supported beam, as the bending moment in the supports is zero, curvatures in concrete slab and steel beam shall also be zero, as shown in Fig. 24.

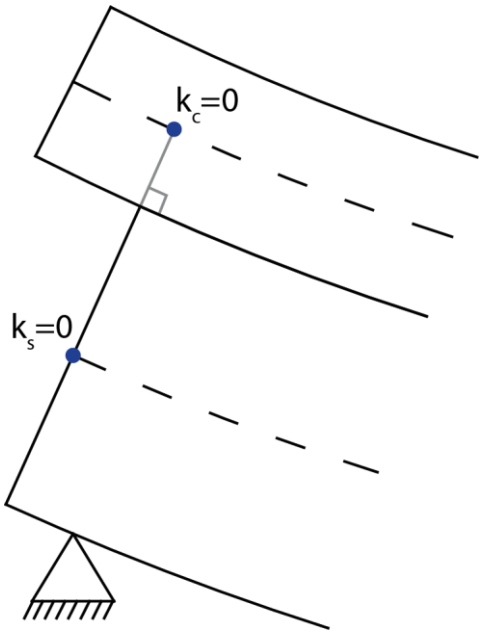

Figure 24. Curvatures of concrete and steel at one simply support

Therefore, the general unknowns, as well as equations, may be adapted to the structural case and reduce the order.

Following are presented the three main equations, for a generic step (ith-step). As it has been said previously, some changes are conducted respect to the general equations (Eqs. (28)-(31)), mostly regarding the calculation of integrals.

1st equation

$$(X_c^i - X_c^{i-1}) \cdot \theta_c^{i-1} + \frac{\kappa_c^i(X_c^i) + 2 \cdot \kappa_c^{i-1}(X_c^{i-1})}{6} \cdot (X_c^i - X_c^{i-1})^2 = (X_s^i - X_s^{i-1}) \cdot \theta_s^{i-1} + \frac{\kappa_s^i(X_s^i) + 2 \cdot \kappa_s^{i-1}(X_s^{i-1})}{6} \cdot (X_s^i - X_s^{i-1})^2 \quad (32)$$

2nd equation

$$X_c^i + h_c \cdot \theta_c^i = X_s^i - h_s \cdot \theta_s^i \tag{33}$$

3rd equation

$$\kappa_s^i(X_s^i) \cdot EI_s + \kappa_c^i(X_s^i) = M_f(X_s^i) \tag{34}$$

where:

$$\kappa_c^i(X_s^i) = \frac{(\kappa_c^i(X_c^i) - \kappa_c^{i-1}(X_c^{i-1}))}{(X_c^i - X_c^{i-1})} \cdot (X_c^i - X_s^{i-1}) + \kappa_c^{i-1}(X_c^{i-1}) \tag{35}$$

$$\theta_c^i = \left[\theta_c^1 + \sum_{j=1}^{i}\left(\frac{\left(\kappa_c^j(X_c^j) + \kappa_c^{j-1}(X_c^{j-1})\right)}{2} \cdot (X_c^j - X_c^{j-1})\right)\right] \tag{36}$$

$$\theta_s^i = \left[\theta_s^1 + \sum_{j=1}^{i}\left(\frac{\left(\kappa_s^j(X_s^j) + \kappa_s^{j-1}(X_s^{j-1})\right)}{2} \cdot (X_s^j - X_s^{j-1})\right)\right] \tag{37}$$

In general, integrals are approximated by using the trapezoidal rule. This type of approximation seems accurate enough if functions are mostly regular, which is the case.

Eqs. (36) and (37) show how rotation along the whole beam is obtained, for concrete and steel beam.

Regarding the third equation, bending moment equilibrium is performed at any cross section defined by steel coordinates. Thus, bending moment in concrete slab is obtained by interpolation.

Also, deflections for concrete slab and steel beam may be calculated when knowing curvatures and rotations. Their expressions are shown in Eqs. (38) and (39).

$$u_c^i = u_c^{i-1} + (X_c^i - X_c^{i-1}) \cdot \theta_c^{i-1} + \frac{\kappa_c^i(X_c^i) + 2 \cdot \kappa_c^{i-1}(X_c^{i-1})}{6} \cdot (X_c^i - X_c^{i-1})^2 \tag{38}$$

$$u_s^i = u_s^{i-1} + (X_s^i - X_s^{i-1}) \cdot \theta_s^{i-1} + \frac{\kappa_s^i(X_s^i) + 2 \cdot \kappa_s^{i-1}(X_s^{i-1})}{6} \cdot (X_s^i - X_s^{i-1})^2 \tag{39}$$

4.3.3 Numerical scaling

Scaling is a very important issue to consider in mathematical computations when using numerical software. A computer stores floating-point numbers with a limited precision because it uses a fixed number of bytes to store them. In some cases, when doing calculations, problems can arise because of this. Especially if operations are done with small and large values, which is the present case. In these situations, the precision of small number may be lost.

The more floating-point calculations are done, the more chance there is that numerical instability occurs and doing calculations with big and small numbers results in faster occurrence of this effect. Then there is also the effect of accumulating rounding errors.

The simplex algorithm is a typical iterating process where factors of thousands of floating calculations are done to find the optimal solution. The chance of numerical instability is then also quite big. But scaling not only improves numerical stability and minimizes rounding errors, it also improves performance. When a model is not scaled, the algorithm could reject certain pivot elements because they are too small and because of this, the solver does not choose the shortest route to the solution. In other words, the algorithm may not take into account some parameters or equations because they may be really small compared to other ones. If a model is proper scaled, this effect will not occur.

Looking at the equations defining the model, it can be seen that first two equations are about displacements, in meters units, whereas third equation is for the equilibrium and its units are kN·m. At the first stages of creating the model, it was proved that, when finding the solution by optimization, the error obtained by the third equation was much bigger than the other two, which means that this equation carried the most weight. In order to obtain a reliable model, all equations shall have similar weight inside the system of equations. Therefore, it is considered to scale the third equation reducing its contribution on the system of equations. In the model, as it is shown in the script, the scaling factor is named by the letter D. The value of the scaling factor depends on the case and it is balanced between precision and the possibility of finding a solution.

4.3.4 Description of the procedure

In this section, it is presented a general step-by-step explanation of the programming procedure of the model. The script can be found in the appendices of the thesis, and complements the information presented next.

1. Definition of physical parameters

First step is to define the physical characteristics of the beam, which are:

Table 1. Physical parameters and nomenclature used in the code

Physical parameter	Matlab nomenclautre
Beam length	*L*
Concrete slab thickness	*H_c*
Steel beam thickness	*H_s*
Young's modulus of concrete, $\boldsymbol{E_c}$	*E_c*
Young's modulus of steel, $\boldsymbol{E_s}$	*E_s*
Moment of inertia of concrete, $\boldsymbol{I_c}$	*I_c*
Moment of inertia of steel, $\boldsymbol{I_s}$	*I_s*
Punctual force, $\boldsymbol{F}$	*F*

2. Definition of numerical parameters

The numerical parameters of the model are:

Table 2. Numerical parameters and nomenclature used in the code

Numerical parameter	Matlab nomenclautre
Number of elements	*n_elem*
Scaling factor	*D*
Tolerance	*tol*

The number of cross sections is the number of elements plus one.

3. Definition of the vector of cross sections at steel centroid

As it is pointed previously, cross sections of steel centroid are defined. Separation between them is the length of the beam divided by the number of elements. In the code, it is named *x_s*. Cross sections are defined by the letter i.

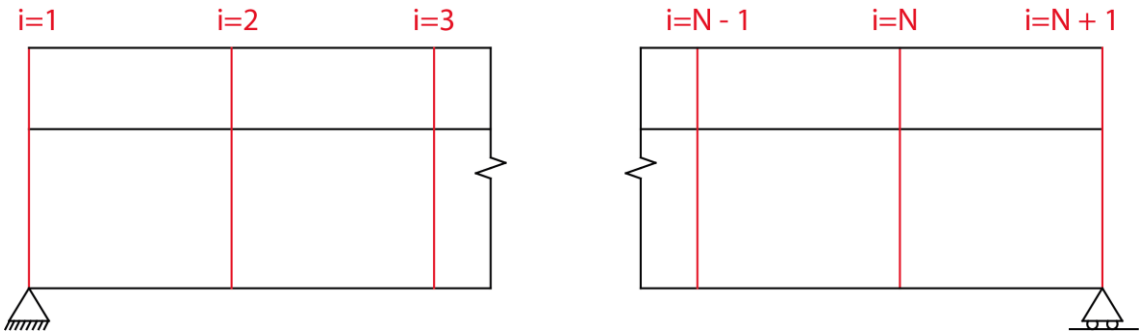

Figure 25. Cross sections definition for a non-deformed shape

4. Calculation of the bending moment at cross sections

It is defined the function *ssb_plmd_i*, to obtain the value of the bending moment for a simply supported beam with a punctual load at mid-span, and gathered in the vector *M*.

5. Definition of the vector of unknowns and the system of equations

The vector X is defined as the vector gathering all the unknowns of the problem, which will be found by optimization. Its dimension is 1 x 3*N+5. It contains the concrete centroid coordinate at cross sections, the concrete curvature and the steel curvature, as well as initial rotations for concrete and steel.

Table 3. Unknowns and nomenclature used in the code

	Matlab nomenclautre
Concrete centroid coordinate, $\boldsymbol{x_c}$	*x_c*
Concrete curvature, $\boldsymbol{k_c}$	*k_c*
Steel curvature, $\boldsymbol{k_S}$	*k_s*
Concrete initial rotation, $\boldsymbol{\theta_c^1}$	*theta_c0*
Steel initial rotation, $\boldsymbol{\theta_s^1}$	*theta_s0*

$$X = (x_c \quad k_c \quad k_S \quad thetha_{c0} \quad theta_{s0})$$

Where:

- x_c is a vector of dimension 1 x N+1
- k_c is a vector of dimension 1 x N+1

- k_S is a vector of dimension 1 x N+1
- θ_c^1 is a scalar
- θ_s^1 is a scalar

As it is shown in Fig.24, curvatures on both supports, for the concrete slab and the steel beam are zero. Therefore, this reduces both vectors of curvatures from dimension 1 x N+1 to 1 x N-1, which means in a reduction of the unknowns from 3*N+5 up to 3*N+1.

Regarding the system of equations to be minimized, it is defined in the code the function *syst_eq,* which applies Eqs. (32)-(34) to any cross section from i=2 to i=N+1. This means 3*N equations. Apart from that, at i=1 (left support of the beam), it will be applied in the optimization, as a restriction, the Eq.(33). Therefore, the total number of equations will be 3*N+1.

Table 4. Equations and unknowns for the problem

Equations	• System of equations defined by Eqs. (33)-(35), at cross sections i, from i=2 to i=N+1 • $\boldsymbol{X_c^1 + h_c \cdot \theta_c^1 + h_s \cdot \theta_s^1 = 0}$	3N+1
Unknowns	• $(X_c^1, \dots, X_c^{N+1})$ • $(\kappa_c^2(X_c^2), \dots, \kappa_c^N(X_c^N))$ • $(\kappa_s^2(X_s^2), \dots, \kappa_s^N(X_s^N))$ • θ_c^1 • θ_s^1	3N+1

6. Optimization

With the established unknowns and equations, it is possible to run the function *fmincon,* to find a solution of vector X which minimizes the system of equations *syst_eq*. To do so, it is needed an initial value of the vector of unknowns, which the closer to the final expected solution the better. It is named *initial_values* in the code.

7. Iterative process of optimization using the while loop to satisfy established conditions

The code finds the solution after running the optimization function *fmincon*. However, the first initial solution does not satisfy that deflections of concrete and steel at the right support must be null. In order to fulfill this condition, it is introduced in the model an iterative mechanism in which, the optimum solution is continually found according to this condition and a tolerance. In other words, optimization is run iteratively, updating initial rotations at each step, until tolerance is fulfilled. This tolerance can be set and is highly relevant, as there must be a balance between a really low tolerance, which may mean not being able to find a solution; or a high tolerance value, which may represent a solution not precise enough.

The way to update initial rotations is:

$$\theta_c^1(step\ m+1) = \theta_c^1(step\ m) - \frac{u_c^{N+1}(step\ m)}{L}$$

$$\theta_s^1(step\ m+1) = \theta_s^1(step\ m) - \frac{u_s^{N+1}(step\ m)}{L}$$

where:

- $\theta_c^1(step\ m+1)$ is the initial rotation for the next step in the concrete slab
- $\theta_s^1(step\ m+1)$ is the initial rotation for the next step in the steel beam
- $\theta_c^1(step\ m)$ is the initial rotation for the currentt step in the concrete slab
- $\theta_s^1(step\ m)$) is the initial rotation for the current step in the steel beam
- $u_c^{N+1}(step\ m)$ is the deflection at the cross section N+1 (right support) of the concrete slab for the current step
- $u_s^{N+1}(step\ m)$ is the deflection at the cross section N+1 (right support) of the steel beam for the current step

8. Final results

Finally, when the solution is precise enough, results may be obtained. The model gives the value of concrete centroid cross section coordinates, concrete curvature and steel curvature and plots them in a serious of graphs. Also, graphs for deflections and rotations can also be drawn.

Regarding curvatures, the code also plots the theoretical curvature, k_t, used for previous researches, which considered that curvatures of concrete and steel where the same. This curvature can be compared with the curvatures of concrete and steel obtained with the model.

$$k_t = \frac{M_f}{EI_s + EI_c} \tag{40}$$

5. APPLICATION OF THE PROPOSED METHOD

5.1 INTRODUCTION

The proposed method is applied, as said, in the case of a simply supported beam. First of all, it is studied the composite beam under a punctual load at mid-span. With this situation, the model will be validated. Next, the model is used to analyze the beam under other types of loads (or another type of load: distributed load) and for different thickness/span relations. These different cases under study represent a parametrical analysis of the problem. It will allow to get a better understanding of the problem and obtain a focus on the important parameters.

5.2 SIMPLY SUPPORTED BEAM UNDER PUNCTUAL LOAD AT MID-SPAN

This is the same case studied by J. Martínez and J. Ortiz and also by J. Turmo et al. in their paper. Hence, results obtained in this case will be compared to the ones obtained in previous research.

5.2.1 Physical parameters

Physical characteristics of the composite beam are shown in Table 5.

Table 5. Characteristics of the composite beam and force applied

Composite beam length	3 m
Concrete slab thickness	0.2 m
Steel beam thickness	0.3 m
Young's modulus of concrete, $\boldsymbol{E_c}$	3.2E7 kN/m^2
Young's modulus of steel, $\boldsymbol{E_s}$	2.1E8 kN/m^2
Moment of inertia of concrete, $\boldsymbol{I_c}$	6.67E-4 m^4
Moment of inertia of steel, $\boldsymbol{I_s}$	8.36E-5 m^4
Punctual force, $\boldsymbol{F}$	100 kN

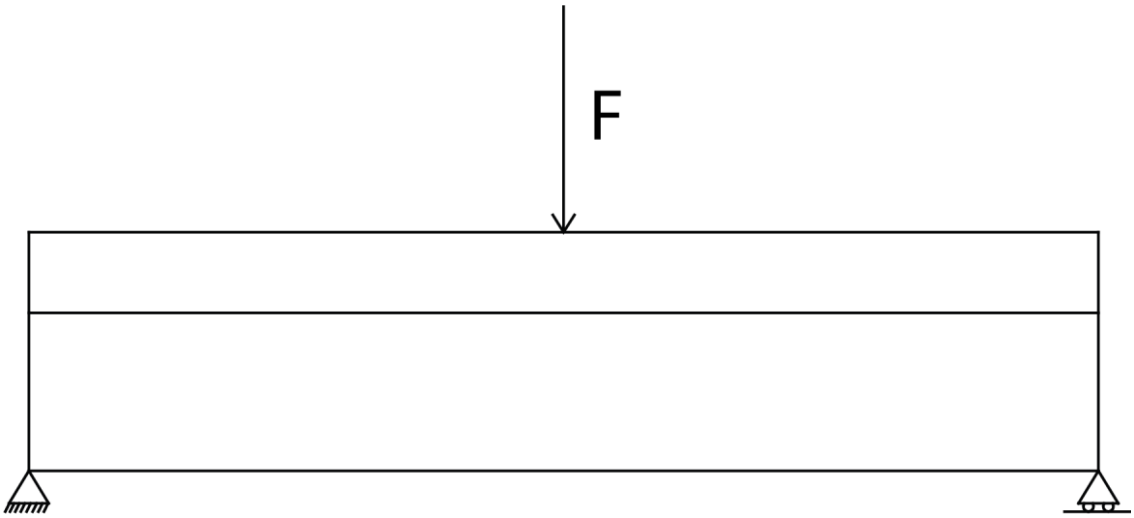

Figure 26. Simply supported beam under punctual load F at mid-span

As it has been stated previously, equations and unknowns adapt depending on the case of study.

5.2.2 Numerical parameters

After establishing the physical parameters of the model, numerical parameters are needed to be studied, to see the behaviour of the model in regards of them, and if possible, reduce its variability.

These factors are:

- The number of elements in which the composite beam is divided, N.
- The scaling factor of the third equation, D.
- The tolerance.

Regarding the scaling factor, in Fig. 27 is shown the value of the errors for each equation at all cross sections, for N=20 and tol= 1E-6, when the scaling factor D is equal to 1. Residue for the third equation is much higher compared to the other two, which proves the need for scaling. Comparing the order of magnitude of the errors, the value of D shall be around 1E-4.

The important issue is to choose a correct value to scale. Different values of D were proved. It was seen, at the end, that the value per se it was not important. What it was relevant was the order of magnitude. Finally, the value of D was established as:

$$D = \frac{1}{E_s \cdot I_s} \tag{41}$$

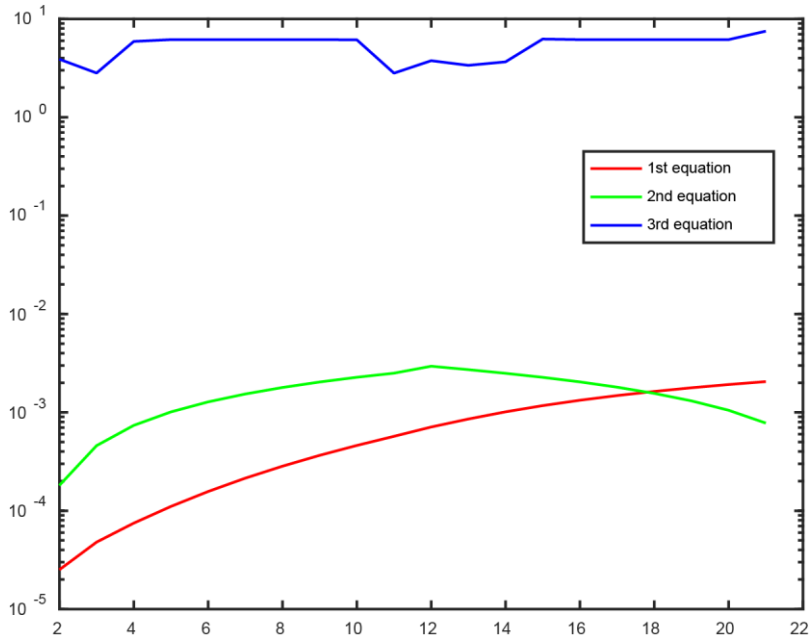

Figure 27. Residues of the three equations when D=1

With this value of D, the model is able to find an enough good solution for different values of tolerances and number of elements. Therefore, this is the value of D chosen. In Fig. 28 are shown the residues in this case. It is seen that all errors are practically of the same order of magnitude, which is the seek performance.

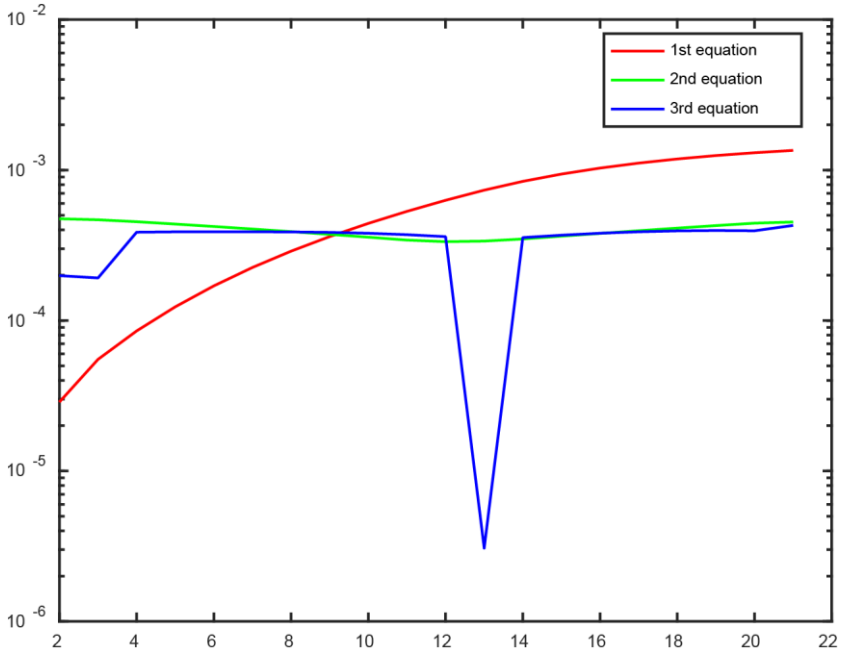

Figure 28. Residues of the three equations for the chosen D

After establishing the scaling factor, the model is analysed for different values of tolerance and number of elements.

Regarding the tolerance, its value will depend on the grade of precision that is wanted for the model and the possibility of the model to find a solution. For a low tolerance, the exactitude

may be high, but the model may be not able to converge. On the other hand, for a high tolerance, the solution may not be considered accurate enough.

About the number of elements, it is clear that the more number of elements, the better performance of the model. This is due to the fact that for large number of elements, the distance between them is small, which means more precise results when using the trapezoidal rule for calculating the integrals; and specially, the theory of strength of materials is better applied, as the difference of rotations from one cross section to the next one is smaller. However, with a large number of elements, the model may be not work due to it is not able to find a solution because the number of calculations is very high. The possibility of finding a solution also depends on the combination of the tolerance and the number of elements.

The model has been run for some different number of elements. In each case, residues of equations have been checked, in order to see the effect on the precision of the model. In Fig. 29 are gathered the results. Firstly, it is important to say that for 60 elements and more, the model is not able to find the minimum of the equation. Residues have been checked for number of elements equal 20, 30, 40 and 50. All three residues stay mainly of the same order, but the trend is that, the more number of elements, the less residue equations present. Therefore, it is considered to consider the maximum number of elements in which the model is able to find a solution.

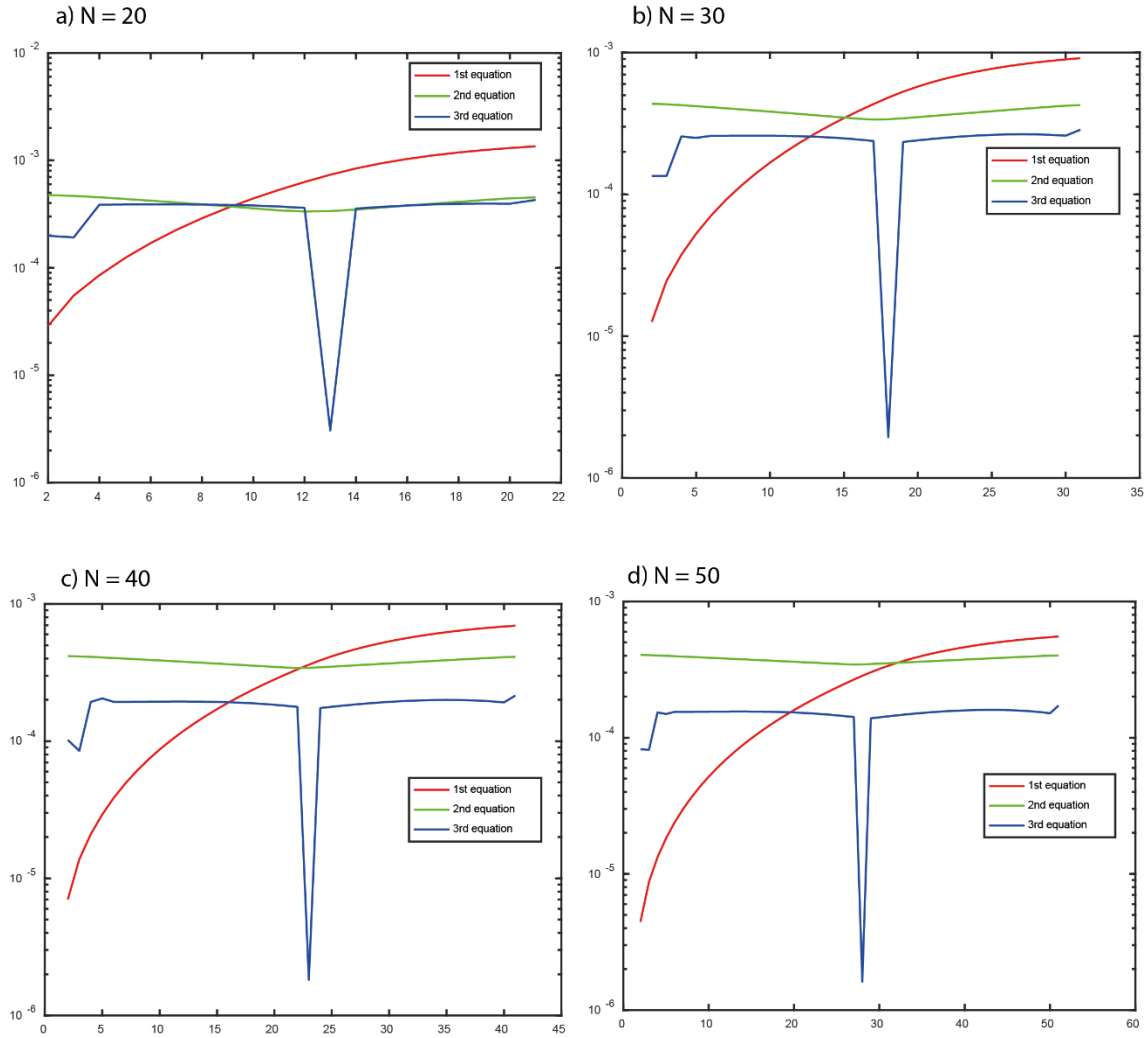

Figure 29. Residues of the three equations for different number of elements

5.2.3 Results

In this section, results obtained by the model for a specific case are presented. A part from using the physical characteristics shown in Tab. XXX, a certain number of elements and tolerance have been chosen, as it can be seen in Table 6.

Table 6. Tolerance and number of elements

Tolerance	1E-6
Number of elements	50

First of all, results obtained are shown in Table 7.

Table 7. Results obtained by the model

i	x_s [m]	x_c [m]	k_c [m^{-1}]	k_S [m^{-1}]
1	0	0.000361485	0.000000E+00	0.000000E+00
2	0.06	0.060361158	7.401788E-05	8.145666E-05
3	0.12	0.120359010356	1.555187E-04	1.532440E-04
4	0.18	0.180356145	2.323584E-04	2.305439E-04
5	0.24	0.240352094	3.093789E-04	3.078736E-04
6	0.3	0.300346888	3.862941E-04	3.852186E-04
7	0.36	0.360340525	4.631294E-04	4.626737E-04
8	0.42	0.420333006	5.398961E-04	5.402111E-04
9	0.48	0.480324329	6.165898E-04	6.178354E-04
10	0.54	0.540314496	6.932202E-04	6.955354E-04
11	0.6	0.600303505	7.698037E-04	7.732910E-04
12	0.66	0.660291356	8.463645E-04	8.510725E-04
13	0.72	0.72027805	9.229351E-04	9.288408E-04
14	0.78	0.780263587	9.995565E-04	1.006546E-03
15	0.84	0.840247966	1.076278E-03	1.084127E-03
16	0.9	0.90023119	1.153159E-03	1.161515E-03
17	0.96	0.960213259	1.230264E-03	1.238628E-03
18	1.02	1.020194173	1.307667E-03	1.315377E-03
19	1.08	1.080173936	1.385447E-03	1.391666E-03
20	1.14	1.140152549	1.463689E-03	1.467393E-03
21	1.2	1.200130016	1.542479E-03	1.542451E-03
22	1.26	1.260106339	1.621904E-03	1.616734E-03
23	1.32	1.320081522	1.702050E-03	1.690140E-03
24	1.38	1.380055569	1.782994E-03	1.762572E-03
25	1.44	1.440028486	1.864804E-03	1.833948E-03
26	1.5	1.500000278	1.947437E-03	1.904323E-03
27	1.56	1.559971993	1.863590E-03	1.835441E-03
28	1.62	1.619944893	1.780614E-03	1.765500E-03
29	1.68	1.679918914	1.698653E-03	1.694321E-03
30	1.74	1.739894061	1.617641E-03	1.621985E-03
31	1.8	1.79987034	1.537540E-03	1.548537E-03
32	1.86	1.859847756	1.458304E-03	1.474035E-03

33	1.92	1.919826312	1.379874E-03	1.398549E-03
34	1.98	1.979806014	1.302188E-03	1.322155E-03
35	2.04	2.039786866	1.225176E-03	1.244939E-03
36	2.1	2.099768871	1.148761E-03	1.166993E-03
37	2.16	2.159752033	1.072864E-03	1.088415E-03
38	2.22	2.219736355	9.973957E-04	1.009312E-03
39	2.28	2.279721838	9.222647E-04	9.297954E-04
40	2.34	2.339708486	8.473702E-04	8.499888E-04
41	2.4	2.399696299	7.726037E-04	7.700241E-04
42	2.46	2.459685279	6.978473E-04	6.900445E-04
43	2.52	2.519675426	6.229730E-04	6.102063E-04
44	2.58	2.57966674	5.478409E-04	5.306793E-04
45	2.64	2.63965922	4.722992E-04	4.516488E-04
46	2.7	2.699652864	3.961829E-04	3.733155E-04
47	2.76	2.759647669	3.193137E-04	2.958959E-04
48	2.82	2.819643633	2.415043E-04	2.196251E-04
49	2.88	2.879640751	1.625262E-04	1.447299E-04
50	2.94	2.939639017	8.217443E-05	7.161766E-05
51	3	2.999638433	0.000000E+00	0.000000E+00

	Initial rotations [rad]
Concrete, $\boldsymbol{\theta_c^1}$	-1.445543E-03
Steel, $\boldsymbol{\theta_s^1}$	-1.446207E-03

Comparing both centroid coordinates, it can be seen that they are practically equal. From i=1 to i=25, which is the left part of the beam, concrete coordinates are a little bit higher than steel coordinates for each cross section, whereas from i=27 to i=51, the right part of the beam, it is the inverse. This result was expected because of the concave form of the beam when bent. The fact that values are almost similar reflects that the deformation is low. This also is important in terms of numerical errors. Being almost the same, curvatures and rotations are small. Therefore, some operations are done with very small values, and it can be a reason why the software may not found results for lower tolerances. In addition, at i=26, which is the cross section at mid-span, both concrete and steel coordinates shall be exactly the same, due to the symmetry of the case. They can be considered equal as they are different at the seventh decimal, which is so small that can be negligible.

Regarding the curvatures, both for concrete and steel are almost equal at respective cross section, but they are different at the fourth or fifth decimal, depending on the cross section. Again, tolerance and numerical error is proved to be playing an important role.

In Table 8 the values of deflections and rotations for both elements are presented.

Table 8. Deflections and rotations

i	$\boldsymbol{u_c}$ **[m]**	$\boldsymbol{u_s}$ **[m]**	$\boldsymbol{\theta_c}$ **[rad]**	$\boldsymbol{\theta_s}$ **[rad]**
1	0.000000E+00	0.000000E+00	-1.445543E-03	-1.446207E-03

2	-8.668769E-05	-8.672356E-05	-1.443322E-03	-1.443763E-03
3	-1.731018E-04	-1.731597E-04	-1.436436E-03	-1.436722E-03
4	-2.589579E-04	-2.590408E-04	-1.424801E-03	-1.425209E-03
5	-3.439757E-04	-3.440919E-04	-1.408550E-03	-1.409056E-03
6	-4.278785E-04	-4.280347E-04	-1.387681E-03	-1.388264E-03
7	-5.103892E-04	-5.105907E-04	-1.362201E-03	-1.362827E-03
8	-5.912316E-04	-5.914810E-04	-1.332114E-03	-1.332740E-03
9	-6.701294E-04	-6.704264E-04	-1.297425E-03	-1.297999E-03
10	-7.468066E-04	-7.471476E-04	-1.258137E-03	-1.258598E-03
11	-8.209877E-04	-8.213649E-04	-1.214254E-03	-1.214533E-03
12	-8.923972E-04	-8.927982E-04	-1.165779E-03	-1.165802E-03
13	-9.607597E-04	-9.611678E-04	-1.112712E-03	-1.112405E-03
14	-1.025800E-03	-1.026194E-03	-1.055051E-03	-1.054343E-03
15	-1.087242E-03	-1.087596E-03	-9.927920E-04	-9.916228E-04
16	-1.144811E-03	-1.145095E-03	-9.259276E-04	-9.242535E-04
17	-1.198229E-03	-1.198413E-03	-8.544463E-04	-8.522492E-04
18	-1.247220E-03	-1.247273E-03	-7.783326E-04	-7.756291E-04
19	-1.291505E-03	-1.291397E-03	-6.975664E-04	-6.944178E-04
20	-1.330806E-03	-1.330512E-03	-6.121228E-04	-6.086460E-04
21	-1.364839E-03	-1.364344E-03	-5.219716E-04	-5.183507E-04
22	-1.393323E-03	-1.392624E-03	-4.270776E-04	-4.235752E-04
23	-1.415972E-03	-1.415085E-03	-3.274002E-04	-3.243689E-04
24	-1.432498E-03	-1.431461E-03	-2.228941E-04	-2.207876E-04
25	-1.442610E-03	-1.441493E-03	-1.135096E-04	-1.128920E-04
26	-1.446015E-03	-1.444923E-03	8.038630E-07	-7.438543E-07
27	-1.442515E-03	-1.441581E-03	1.150808E-04	1.114491E-04
28	-1.432311E-03	-1.431632E-03	2.243575E-04	2.194773E-04
29	-1.415702E-03	-1.415329E-03	3.286903E-04	3.232719E-04
30	-1.392983E-03	-1.392926E-03	4.281380E-04	4.227611E-04
31	-1.364443E-03	-1.364685E-03	5.227560E-04	5.178767E-04
32	-1.330372E-03	-1.330869E-03	6.125975E-04	6.085539E-04
33	-1.291053E-03	-1.291748E-03	6.977124E-04	6.947314E-04
34	-1.246769E-03	-1.247593E-03	7.781470E-04	7.763525E-04
35	-1.197799E-03	-1.198678E-03	8.539438E-04	8.533653E-04
36	-1.144419E-03	-1.145282E-03	9.251405E-04	9.257233E-04
37	-1.086905E-03	-1.087685E-03	9.917706E-04	9.933855E-04
38	-1.025530E-03	-1.026170E-03	1.053862E-03	1.056317E-03
39	-9.605638E-04	-9.610223E-04	1.111438E-03	1.114491E-03
40	-8.922780E-04	-8.925272E-04	1.164515E-03	1.167884E-03
41	-8.209414E-04	-8.209721E-04	1.213105E-03	1.216484E-03
42	-7.468232E-04	-7.466450E-04	1.257210E-03	1.260287E-03
43	-6.701922E-04	-6.698336E-04	1.296828E-03	1.299294E-03
44	-5.913178E-04	-5.908253E-04	1.331947E-03	1.333521E-03
45	-5.104704E-04	-5.099063E-04	1.362548E-03	1.362990E-03
46	-4.279219E-04	-4.273609E-04	1.388600E-03	1.387739E-03

Model validation for composite structures with partial interaction

47	-3.439462E-04	-3.434710E-04	1.410063E-03	1.407816E-03
48	-2.588202E-04	-2.585152E-04	1.426886E-03	1.423281E-03
49	-1.728239E-04	-1.727679E-04	1.439006E-03	1.434212E-03
50	-8.624165E-05	-8.649857E-05	1.446347E-03	1.440702E-03
51	6.369392E-07	2.951672E-08	1.448812E-03	1.442851E-03

Besides, graphs can be plotted. From Tables. 7 and 8 and the plotted graphs, some conclusions may be extracted. Deflections are shown in Fig. 30. Overall, it is important to point that both deflections are mostly equal, as expected. Besides, the deflected shape is symmetric, which is consistent.

Rotations are shown in Fig. 31. According to the symmetry of the structure, rotations at both edges shall be equal but with different sign. This condition is not applied in the model, as it is sought that the model fulfils this condition by itself. It seems that the model fulfils this condition.

Finally, curvatures are plotted in Fig.32. Curvatures of concrete and steel are slightly different, as expected, though the difference is small (around 1E-6, 1E-7 m^{-1}, depending on the cross section). Apart from these curvatures obtained with the model, the theoretical curvature is also shown. Comparing curvatures from the model to the theoretical curvature (the one considered in previous models), they three are almost equal. Differences are around 1E-6, 1E-7 m^{-1},again, and also depending on the cross section. Fig. 33 is a zoom of the curvatures graph and this difference is noticed. Plus, it is seen that the theoretical curvature elapses between steel and concrete curvatures and curvature of concrete is higher than the curvature of steel, as the radius of curvature is smaller, due to the concave bent form and concrete is located on the steel.

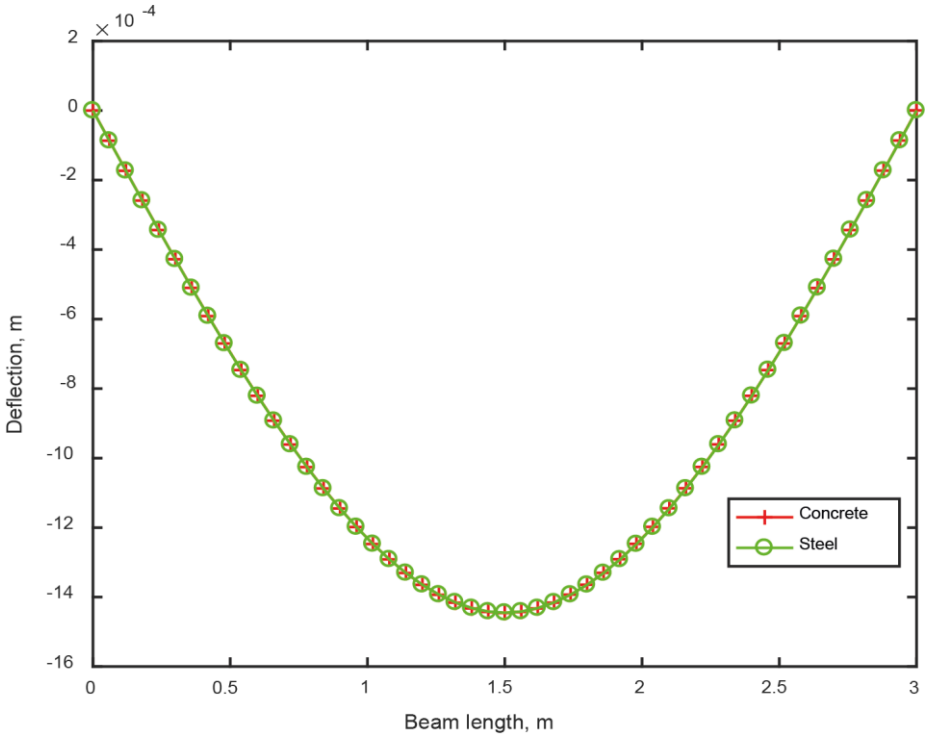

Figure 30. Deflections for a simply supported beam under load at mid-span

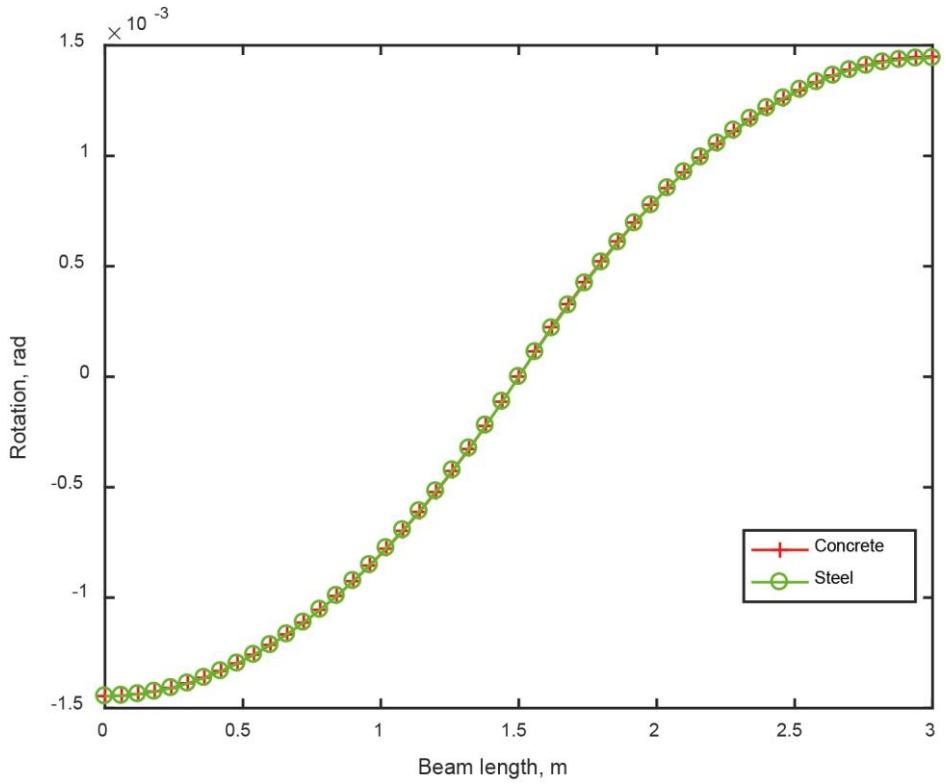

Figure 31. Rotations for a simply supported beam under load at mid-span

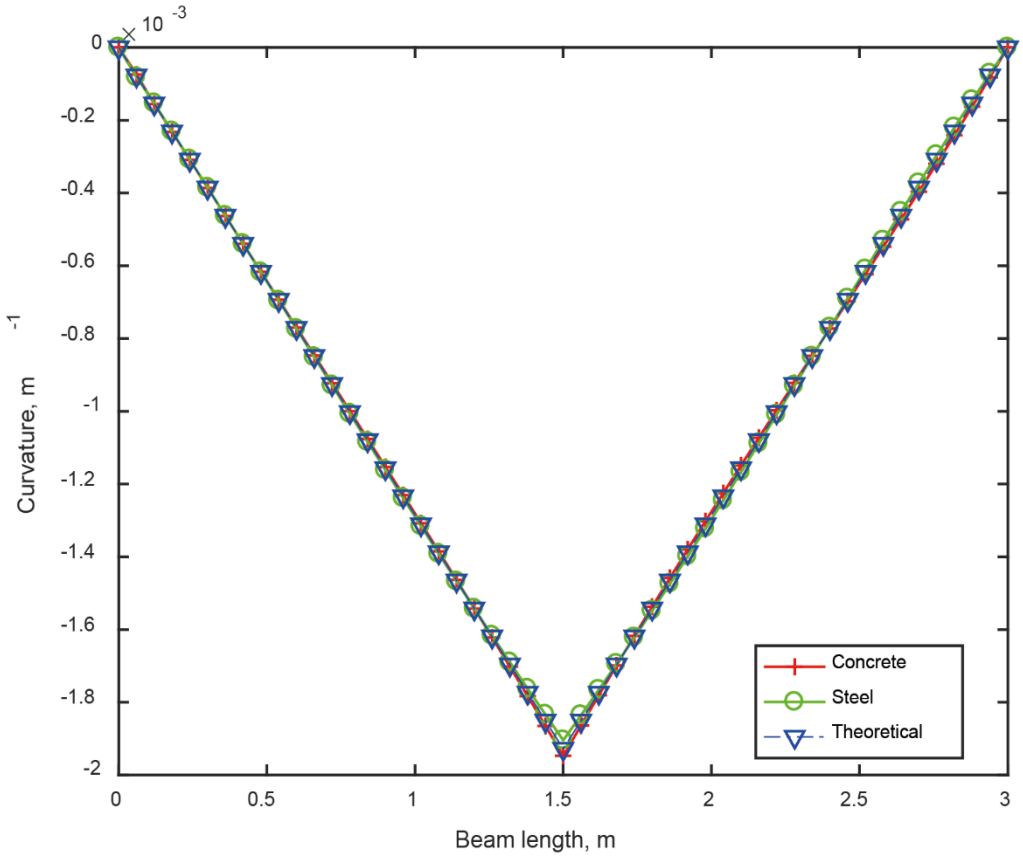

Figure 32. Curvatures for a simply supported beam under load at mid-span

<u>Model validation for composite structures with partial interaction</u>

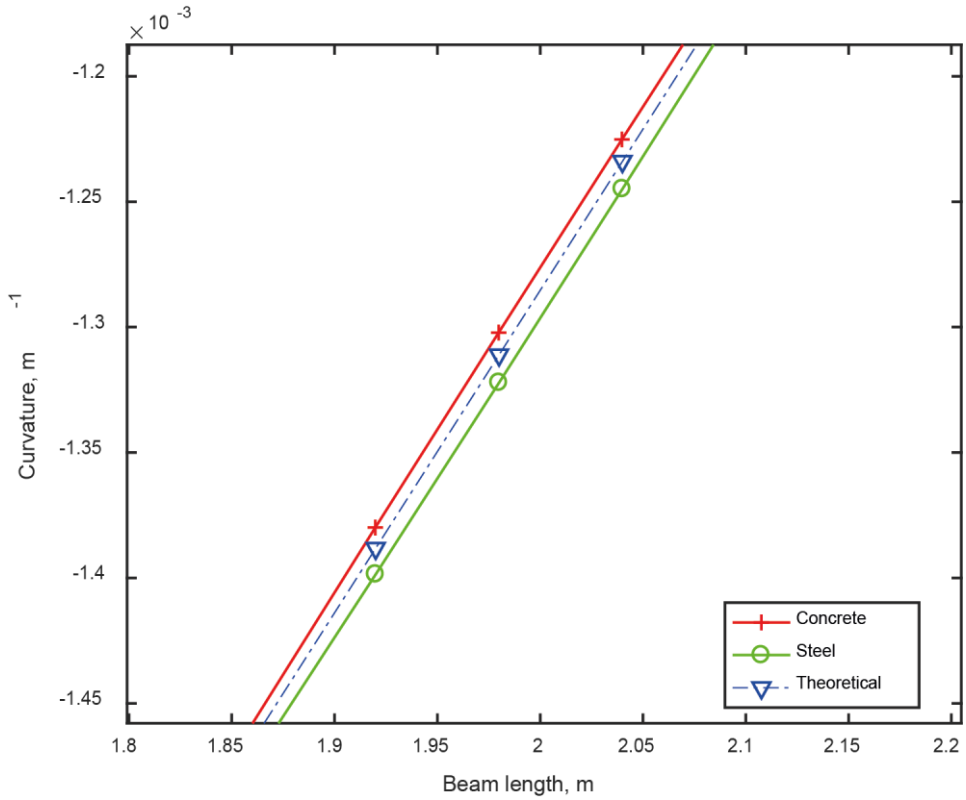

Figure 33. Detail of curvatures for a simply supported beam under load at mid-span

5.3 SIMPLY SUPPORTED BEAM UNDER DISTRIBUTED LOAD

It is sought to test the model under a different type of load, in order to see the influence that different loads may have on it. The case is about a distributed load q applied on the concrete slab, vertical and in the direction of gravity.

5.3.1 Physical parameters

Physical characteristics of the beam are the same as previously.

Table 9. Characteristics of the composite beam and force applied

Composite beam length	3 m
Concrete slab thickness	0.2 m
Steel beam thickness	0.3 m
Young's modulus of concrete, $\boldsymbol{E_c}$	3.2E7 kN/m^2
Young's modulus of steel, $\boldsymbol{E_s}$	2.1E8 kN/m^2
Moment of inertia of concrete, $\boldsymbol{I_c}$	6.67E-4 m^4
Moment of inertia of steel, $\boldsymbol{I_s}$	8.36E-5 m^4
Distributed load, $\boldsymbol{q}$	100 kN/m

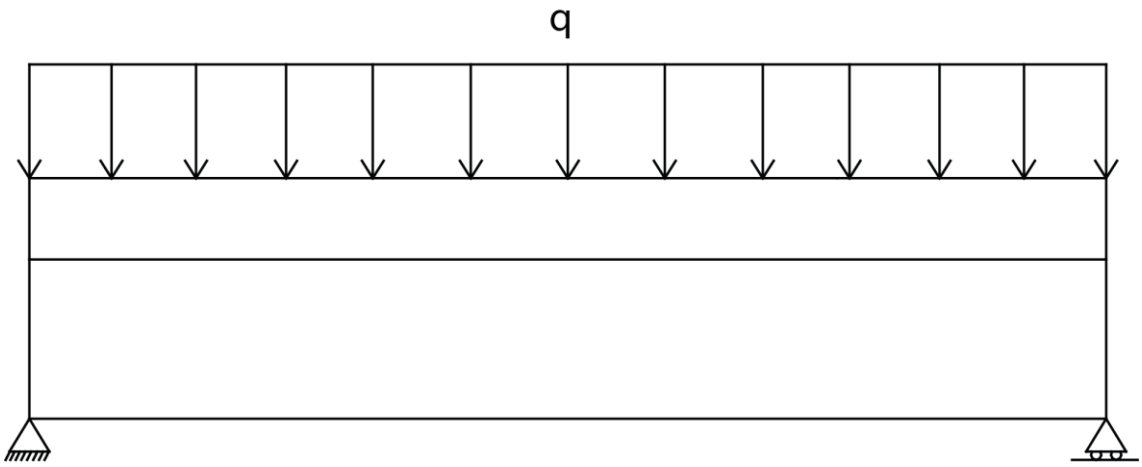

Figure 34. Simply supported beam under distributed load q

5.3.2 Numerical parameters

Numerical parameters are the same as in the case of a punctual load applied, in order to have the same conditions as the previous case, except for the type of load.

Table 10. Numerical parameters

Tolerance	1E-6
Scaling factor	$\frac{1}{E_S \cdot I_S}$
Number of elements	40

5.3.3 Results

First of all, results obtained are shown in Table 11.

Table 11. Results obtained by the model

i	x_s [m]	x_c [m]	k_c [m^{-1}]	k_S [m^{-1}]
1	0	0.000722535	0.000000E+00	0.000000E+00
2	0.075	0.075719581	2.850986E-04	2.814331E-04
3	0.15	0.150712315	5.524737E-04	5.487945E-04
4	0.225	0.225699634	8.037059E-04	8.036930E-04
5	0.3	0.300682317	1.041018E-03	1.043961E-03
6	0.375	0.375660658	1.263819E-03	1.269503E-03
7	0.45	0.450634927	1.472395E-03	1.480178E-03
8	0.525	0.525605398	1.666982E-03	1.675904E-03
9	0.6	0.600572345	1.847607E-03	1.856562E-03
10	0.675	0.675536042	2.014286E-03	2.022141E-03
11	0.75	0.750496764	2.166978E-03	2.172694E-03
12	0.825	0.825454784	2.305599E-03	2.308324E-03
13	0.9	0.900410376	2.430034E-03	2.429177E-03
14	0.975	0.975363812	2.540143E-03	2.535425E-03
15	1.05	1.050315363	2.635773E-03	2.627254E-03

16	1.125	1.1252653	2.716775E-03	2.704852E-03
17	1.2	1.200213893	2.783005E-03	2.768392E-03
18	1.275	1.275161409	2.834343E-03	2.818023E-03
19	1.35	1.350108117	2.870698E-03	2.853857E-03
20	1.425	1.425054284	2.892017E-03	2.875959E-03
21	1.5	1.500000178	2.898291E-03	2.884340E-03
22	1.575	1.574946065	2.889560E-03	2.878951E-03
23	1.65	1.649892213	2.865915E-03	2.859681E-03
24	1.725	1.724838891	2.827497E-03	2.826357E-03
25	1.8	1.799786368	2.774494E-03	2.778749E-03
26	1.875	1.874734915	2.707129E-03	2.716585E-03
27	1.95	1.949684804	2.625652E-03	2.639557E-03
28	2.025	2.024636309	2.530322E-03	2.547348E-03
29	2.1	2.099589706	2.421388E-03	2.439654E-03
30	2.175	2.17454527	2.299061E-03	2.316217E-03
31	2.25	2.249503281	2.163486E-03	2.176855E-03
32	2.325	2.324464017	2.014714E-03	2.021508E-03
33	2.4	2.399427755	1.852663E-03	1.850273E-03
34	2.475	2.474394774	1.677085E-03	1.663451E-03
35	2.55	2.549365349	1.487533E-03	1.461584E-03
36	2.625	2.62433975	1.283328E-03	1.245493E-03
37	2.7	2.699318245	1.063564E-03	1.016322E-03
38	2.775	2.774301093	8.269690E-04	7.754590E-04
39	2.85	2.849288546	5.721904E-04	5.247697E-04
40	2.925	2.924280845	2.959210E-04	2.684349E-04
41	3	2.999278254	0.000000E+00	0.000000E+00

	Initial rotations [rad]
Concrete, $\boldsymbol{\theta_c^1}$	-0.001445543
Steel, $\boldsymbol{\theta_s^1}$	-0.001446207

Looking at results, it is seen in general terms that they present some parallelisms with the case of a punctual load. Comparing both centroid coordinates, it can be seen that they are practically equal. From i=1 to i=20, which is the left part of the beam, concrete coordinates are a little bit higher than steel coordinates for each cross section, whereas from i=22 to i=41, the right part of the beam, it is the inverse. This result was expected because of the concave form of the beam when bent. The fact that values are almost similar reflects that the deformation is low. This also is important in terms of numerical errors. Being almost the same, curvatures and rotations are small. Therefore, some operations are done with very small values, and it can be a reason why the software may not found results for lower tolerances. In addition, at i=21, which is the cross section at mid-span, both concrete and steel coordinates shall be exactly the same, due to the symmetry of the case. They can be considered equal as they are different at the seventh decimal, which is so small that can be negligible.

Regarding the curvatures, both for concrete and steel are almost equal at respective cross section, but they are different at the fourth or fifth decimal, depending on the cross section. Again, tolerance and numerical error is proved to be playing an important role.

In Table 12 the values of deflections and rotations for both elements are presented.

Table 12. Deflections and rotations

i	u_c [m]	u_s [m]	θ_c [rad]	θ_s [rad]
1	0.000000E+00	0.000000E+00	-2.889996E-03	-2.890238E-03
2	-2.164739E-04	-2.165040E-04	-2.879306E-03	-2.879685E-03
3	-4.313486E-04	-4.314382E-04	-2.847900E-03	-2.848551E-03
4	-6.431162E-04	-6.432971E-04	-2.797052E-03	-2.797833E-03
5	-8.503649E-04	-8.506489E-04	-2.727890E-03	-2.728546E-03
6	-1.051763E-03	-1.052142E-03	-2.641484E-03	-2.641791E-03
7	-1.246059E-03	-1.246509E-03	-2.538911E-03	-2.538678E-03
8	-1.432082E-03	-1.432563E-03	-2.421231E-03	-2.420325E-03
9	-1.608741E-03	-1.609204E-03	-2.289492E-03	-2.287857E-03
10	-1.775022E-03	-1.775417E-03	-2.144741E-03	-2.142406E-03
11	-1.929991E-03	-1.930269E-03	-1.988026E-03	-1.985100E-03
12	-2.072792E-03	-2.072914E-03	-1.820398E-03	-1.817062E-03
13	-2.202647E-03	-2.202588E-03	-1.642917E-03	-1.639405E-03
14	-2.318861E-03	-2.318611E-03	-1.456651E-03	-1.453233E-03
15	-2.420814E-03	-2.420387E-03	-1.262679E-03	-1.259632E-03
16	-2.507973E-03	-2.507397E-03	-1.062093E-03	-1.059678E-03
17	-2.579883E-03	-2.579206E-03	-8.559924E-04	-8.544316E-04
18	-2.636173E-03	-2.635456E-03	-6.454892E-04	-6.449410E-04
19	-2.676556E-03	-2.675867E-03	-4.317022E-04	-4.322455E-04
20	-2.700828E-03	-2.700239E-03	-2.157555E-04	-2.173774E-04
21	-2.708870E-03	-2.708445E-03	1.224428E-06	-1.366219E-06
22	-2.700647E-03	-2.700441E-03	2.181122E-04	2.147572E-04
23	-2.676207E-03	-2.676255E-03	4.337876E-04	4.299559E-04
24	-2.635683E-03	-2.635997E-03	6.471387E-04	6.431824E-04
25	-2.579290E-03	-2.579854E-03	8.570663E-04	8.533738E-04
26	-2.507325E-03	-2.508094E-03	1.062486E-03	1.059449E-03
27	-2.420165E-03	-2.421067E-03	1.262332E-03	1.260304E-03
28	-2.318265E-03	-2.319207E-03	1.455556E-03	1.454813E-03
29	-2.202160E-03	-2.203032E-03	1.641130E-03	1.641826E-03
30	-2.072461E-03	-2.073149E-03	1.818042E-03	1.820171E-03
31	-1.929852E-03	-1.930253E-03	1.985293E-03	1.988661E-03
32	-1.775094E-03	-1.775127E-03	2.141894E-03	2.146100E-03
33	-1.609021E-03	-1.608644E-03	2.286850E-03	2.291291E-03
34	-1.432541E-03	-1.431768E-03	2.419158E-03	2.423056E-03
35	-1.246640E-03	-1.245550E-03	2.537784E-03	2.540245E-03
36	-1.052381E-03	-1.051124E-03	2.641656E-03	2.641760E-03
37	-8.509125E-04	-8.497034E-04	2.729639E-03	2.726578E-03
38	-6.434682E-04	-6.425775E-04	2.800518E-03	2.793770E-03

39	-4.313782E-04	-4.310988E-04	2.852978E-03	2.842529E-03
40	-2.160768E-04	-2.166735E-04	2.885529E-03	2.872274E-03
41	8.852023E-07	-7.496510E-07	2.896625E-03	2.882340E-03

Besides, graphs can be plotted. From Tables 11 and 12 and the plotted graphs, some conclusions may be extracted. Deflections are shown in Fig. 35. Overall, it is important to point that both deflections are mostly equal, as expected. Besides, the deflected shape is symmetric, which is consistent. At right support (i=41), deflections are not exactly zero, but it can be considered as null because it is smaller than the chosen tolerance.

Rotations are shown in Fig. 36. According to the symmetry of the structure, rotations at both edges shall be equal but with different sign. This condition is not applied in the model, as it is sought that the model fulfils this condition by itself. It seems that the model fulfils this condition.

Finally, curvatures are plotted in Fig. 37. Curvatures of concrete and steel are slightly different, as expected, though the difference is small. Apart from these curvatures obtained with the model, the theoretical curvature is also shown. Comparing curvatures from the model to the theoretical curvature (the one considered in previous models), they three are almost equal. Fig. 38 is a zoom of the curvatures graph and this difference is noticed. Plus, it is seen that the theoretical curvature elapses between steel and concrete curvatures and curvature of concrete is higher than the curvature of steel, as the radius of curvature is smaller, due to the concave bent form and concrete is located on the steel.

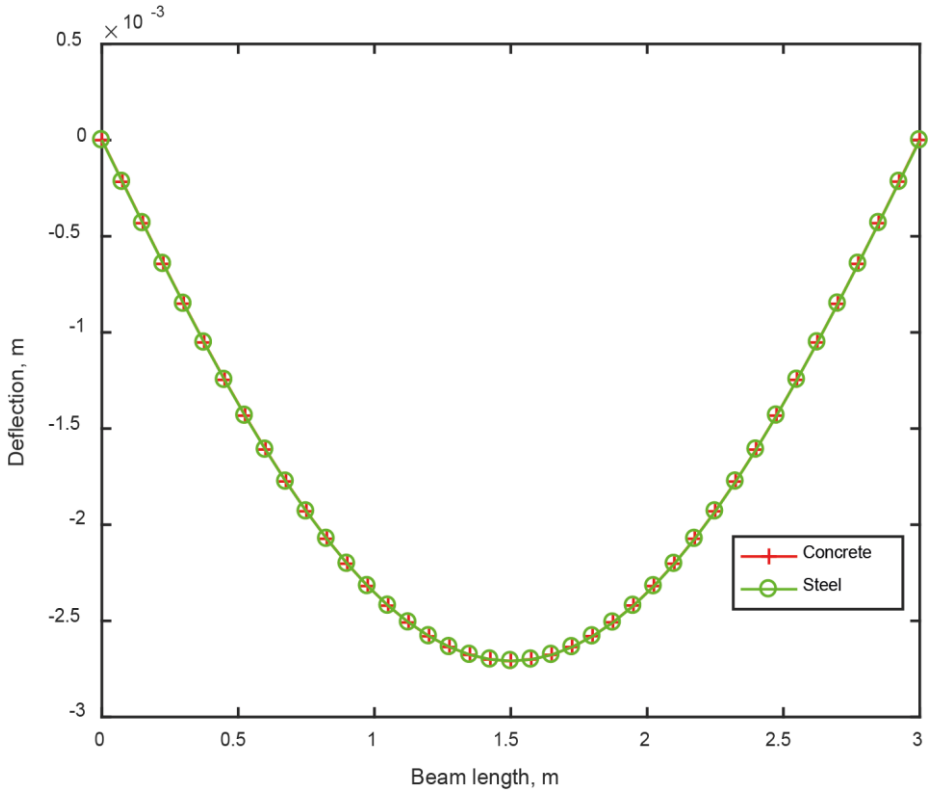

Figure 35. Deflections for a simply supported beam under distributed load

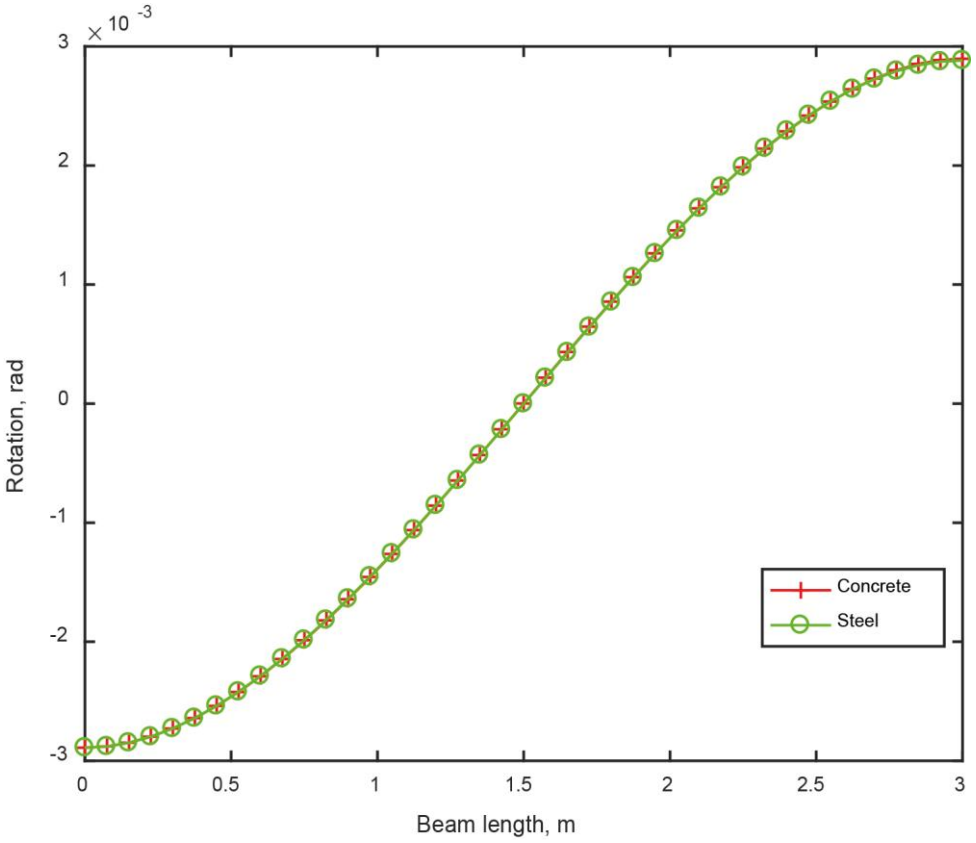

Figure 36. Rotations for a simply supported beam under distributed load

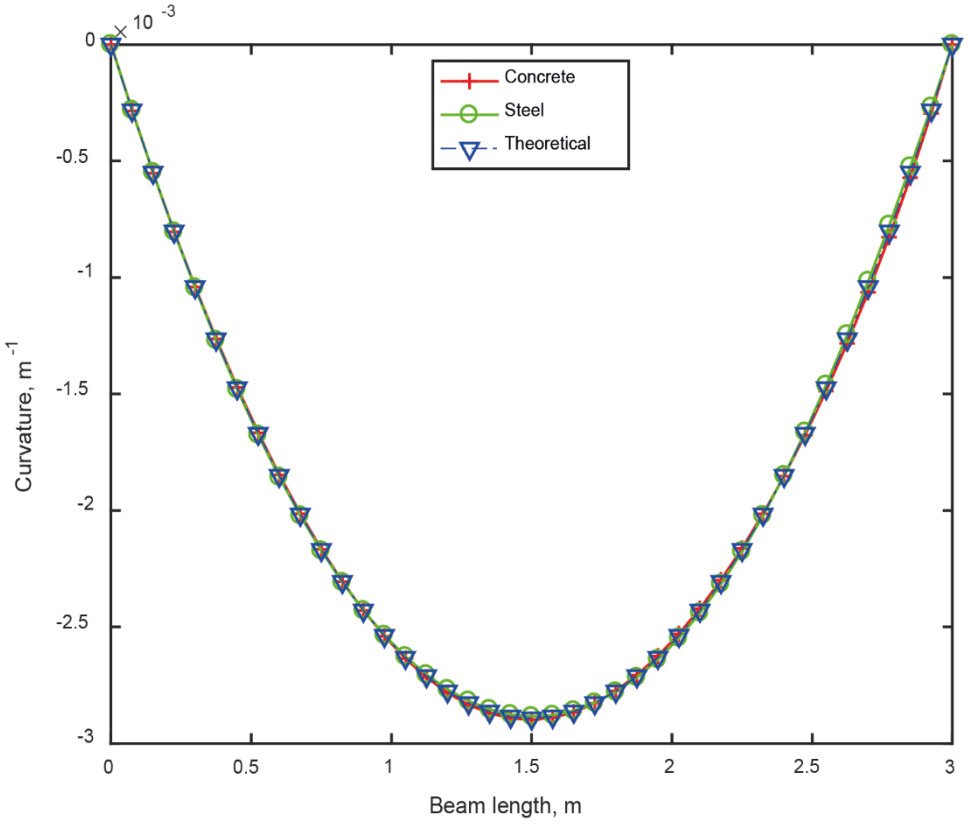

Figure 37. Curvatures for a simply supported beam under distributed load

Model validation for composite structures with partial interaction

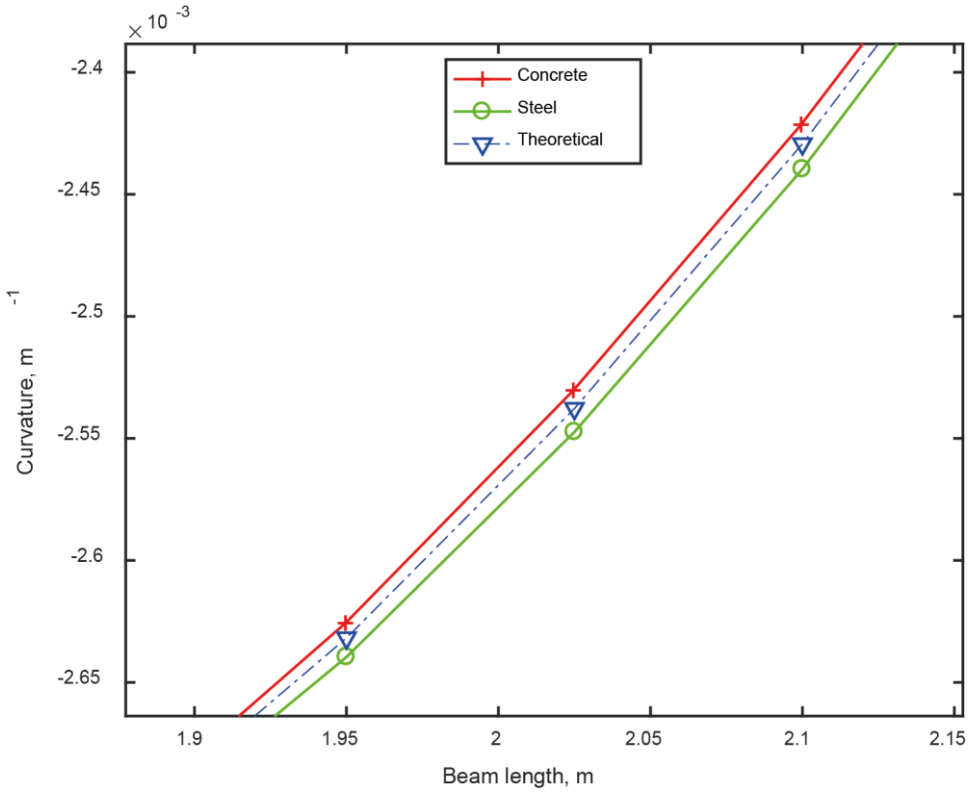

Figure 38. Detail of curvatures for a simply supported beam under distributed load

5.4 ANALYSIS OF A SIMPLY SUPPORTED BEAM WITH DIFFERENT THICKNESS/SPAN RELATIONS

5.4.1 Introduction

This analysis is conducted in order to see the importance of the characteristics of the structure in the problem to study and the behavior of the model in front such variations. The structure is a simply supported composite beam under a punctual load at mid-span of 100 kN.

The reference case is the one presented previously in part 5.2, and from it different cases are analyzed. These cases are summarized in the Tables 14 and 15. It is important to notice that when variating the beam span, stiffness of the beam has remained the same as the reference case. In contrast, when variating the beam thickness (therefore, the stiffness of the beam), the beam span has remained equal to the reference case. In these latter variations, thickness has been changed by combining different thickness of concrete slab and steel beam. A notation (#) has been given to any case, to ease the presentation of the results. The term relation stands for the thickness divided by the span.

Table 13. Reference beam case

#	Concrete thickness [m]	Steel thickness [m]	Total thickness [m]	Span [m]	Relation
R	0.2	0.3 (IPE 300)	0.5	3	0.1667

Table 14. Composite beams with different spans

Variation of beam span					
#	Concrete thickness [m]	Steel thickness [m]	Total thickness [m]	Span [m]	Relation
1	0.2	0.3 (IPE 300)	0.5	5	0.1
2	0.2	0.3 (IPE 300)	0.5	10	0.05
3	0.2	0.3 (IPE 300)	0.5	15	0.0333
4	0.2	0.3 (IPE 300)	0.5	20	0.025

Table 15. Composite beams with different thicknesses

Variation of beam thickness					
#	Concrete thickness [m]	Steel thickness [m]	Total thickness [m]	Span [m]	Relation
5	0.2	0.2 (IPE200)	0.4	3	0.133
6	0.1	0.3 (IPE 300)	0.4	3	0.133
7	0.14	0.36 (IPE360)	0.5	3	0.1667
8	0.3	0.2 (IPE200)	0.5	3	0.1667

5.4.2 Beams with different spans

The model is run for different beam spans, maintaining the thickness of the reference case. A total of 4 different composite beams are tested, with lengths of 5, 10, 15 and 20 m. In all cases, the scaling factor is the same as in the reference case. In Table 16 tolerances and number of elements are shown for each case.

Table 16. Tolerances and number of elements

#	Span	Tolerance	Number of elements
1	5 m	1E-6	40
2	10 m	1E-6	30
3	15 m	1E-6	16
4	20 m	1E-6	14

The longer the beam span, the less number of elements the model can process to find the optimum solution if tolerance remains equal. Other approximation could have been to try for each beam span fewer tolerances but with larger number of elements. In this case, what was wanted is to maintain tolerance the same.

a) Residues

Fig. 39 shows the value of the residue of equations for the 4 beams. It can be seen that the larger the span, the higher the residues of the optimization. Thus, this model may be no consistent for beams with large spans, at errors can be considered too high.

b) Deflections

Fig. 40 present deflections on each case. In each one of them, the deflection on the right support was lower than the established tolerance.

c) Curvatures

Regarding curvatures, which are shown in Fig. 41, in all cases curvatures of concrete and steel are almost equal as the theoretical one. Therefore, it can be said that, despite of the increase on the residues for larger spans, curvatures remain almost the same. In the case of the beam of 10 m span, (Fig. 40 b)), at the first cross sections it appears an oscillation of concrete and steel curvatures. Afterwards, for next cross sections, it disappears.

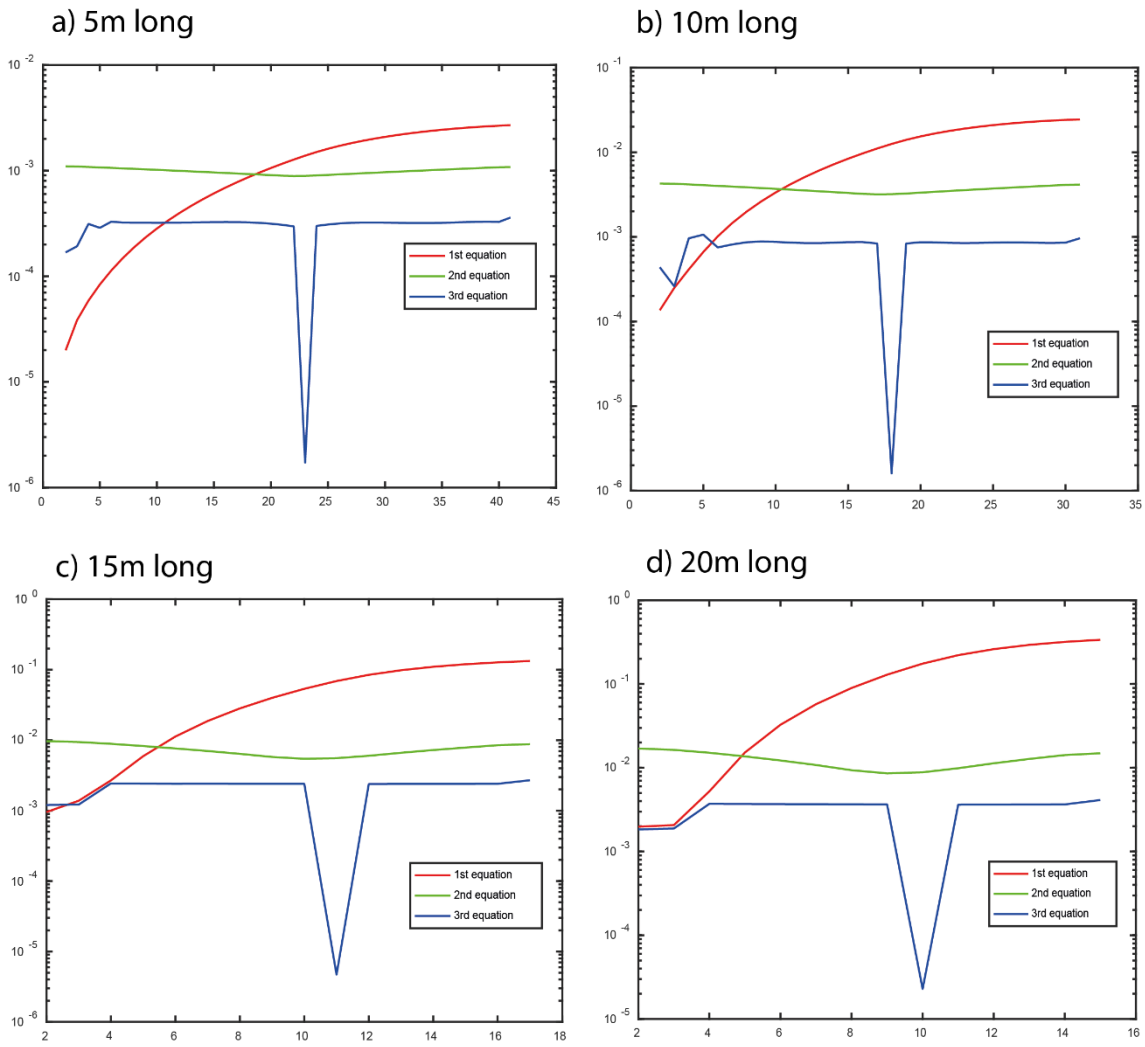

Figure 39. Residues of equations for beams #1 to #4

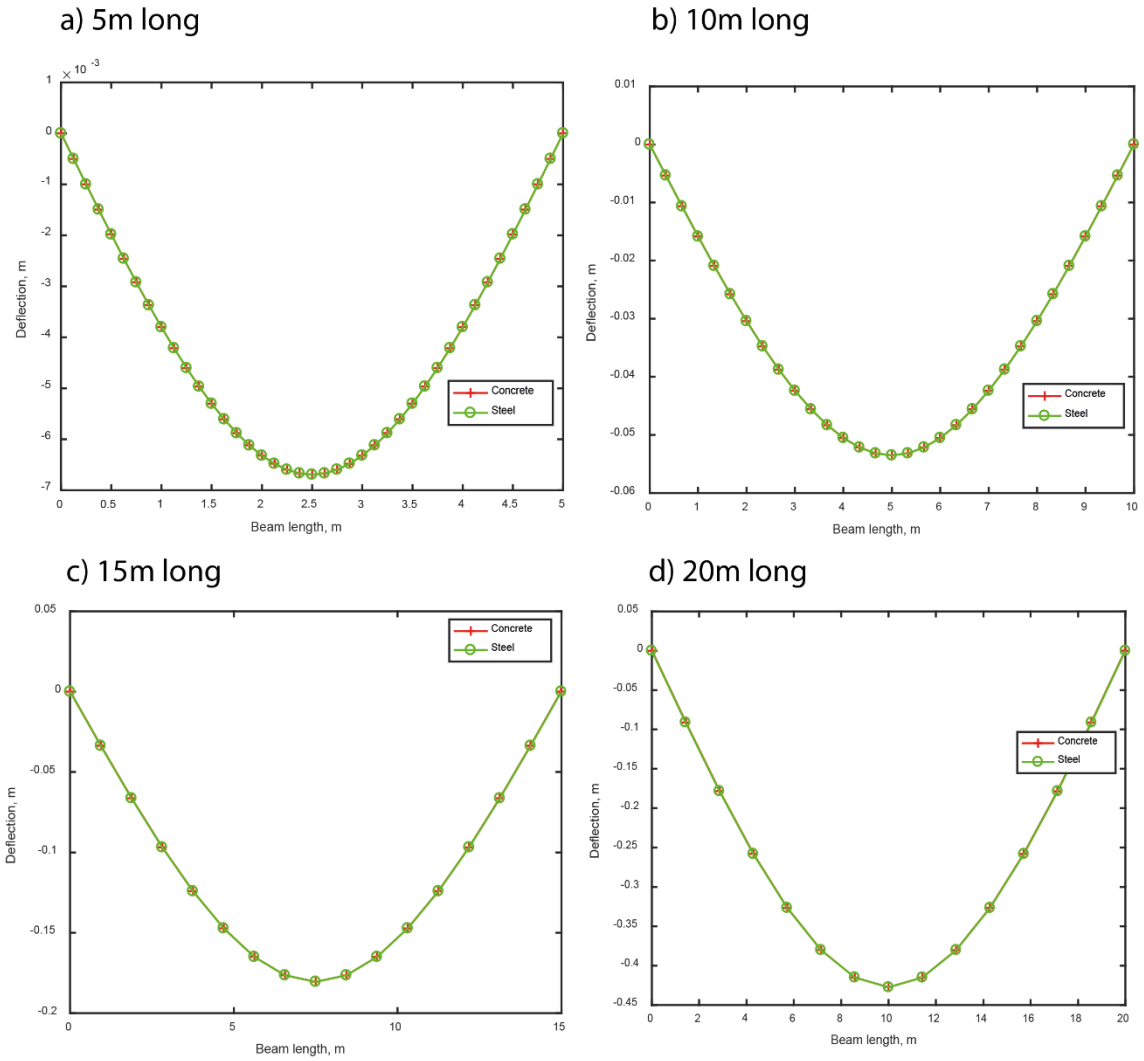

Figure 40. Deflections for beams #1 to #4

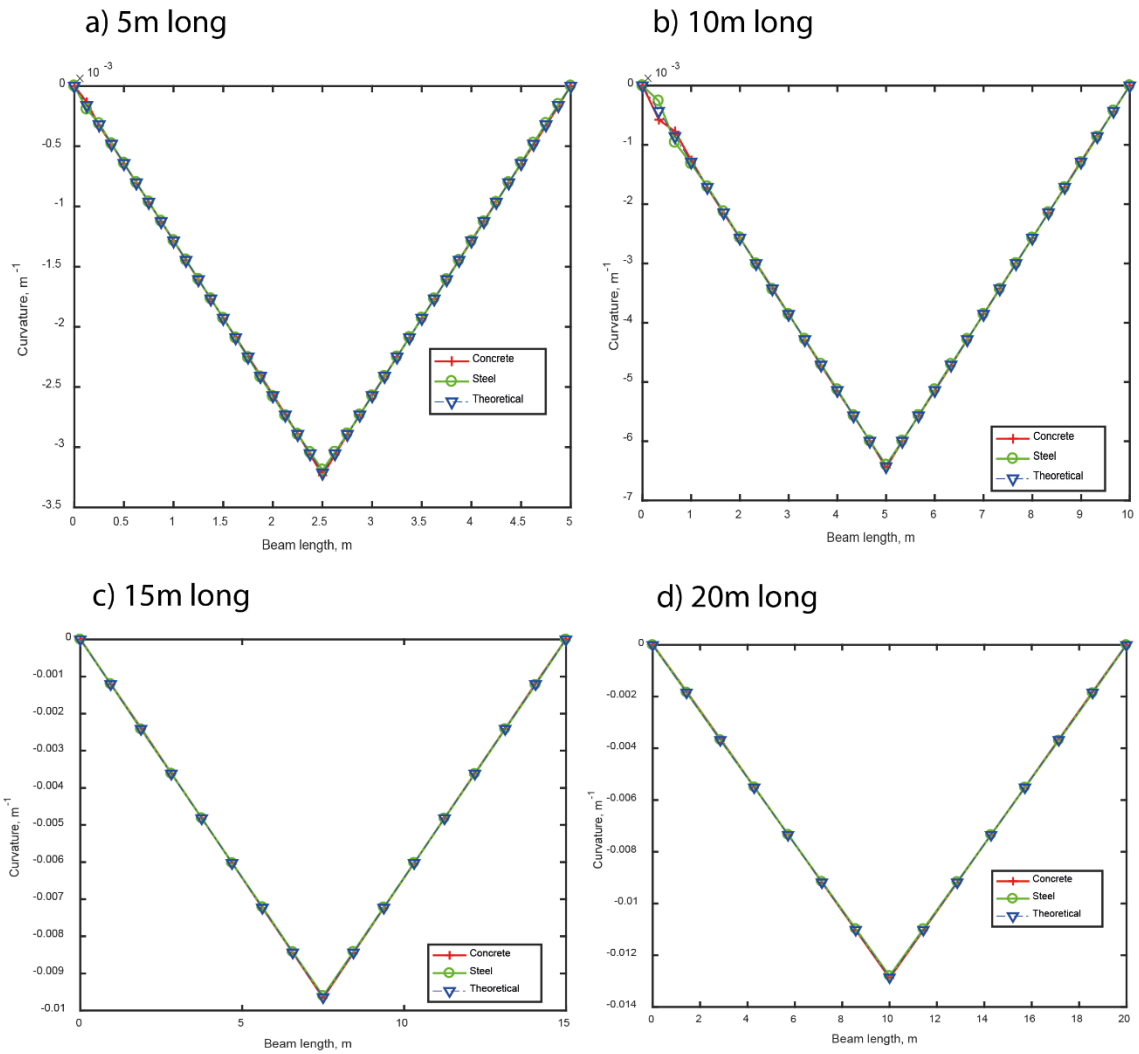

Figure 41. Curvatures for beams #1 to #4

5.4.3 Beams with different thicknesses

A total of 4 different composite beams, with the same length as the reference case (3 m), but with different thicknesses have been calculate with the model. The analysis is divided in two parts: the first part compares two composite beams with 0.4 m of total thickness; the second part compares three composite beams with 0.5 m of total thickness.

a) 0.4 m thickness - # 5 and # 6

Deflections are shown in Fig. 42. Even though both beams have the same total thickness, beam #5 has less deformation due to the higher contribution of the concrete to the bending resistance. In addition, deflections of concrete and steel of each beam are the same.

Curvatures are plotted in Fig. 43. It can be noticed that, for both beams, at mid-span, calculated curvatures from the model does not coincide with the theoretical one. In the beam #5, it is the steel curvature which has a little oscillation. On the other hand, in the beam #6, it is the concrete curvature which has this behavior.

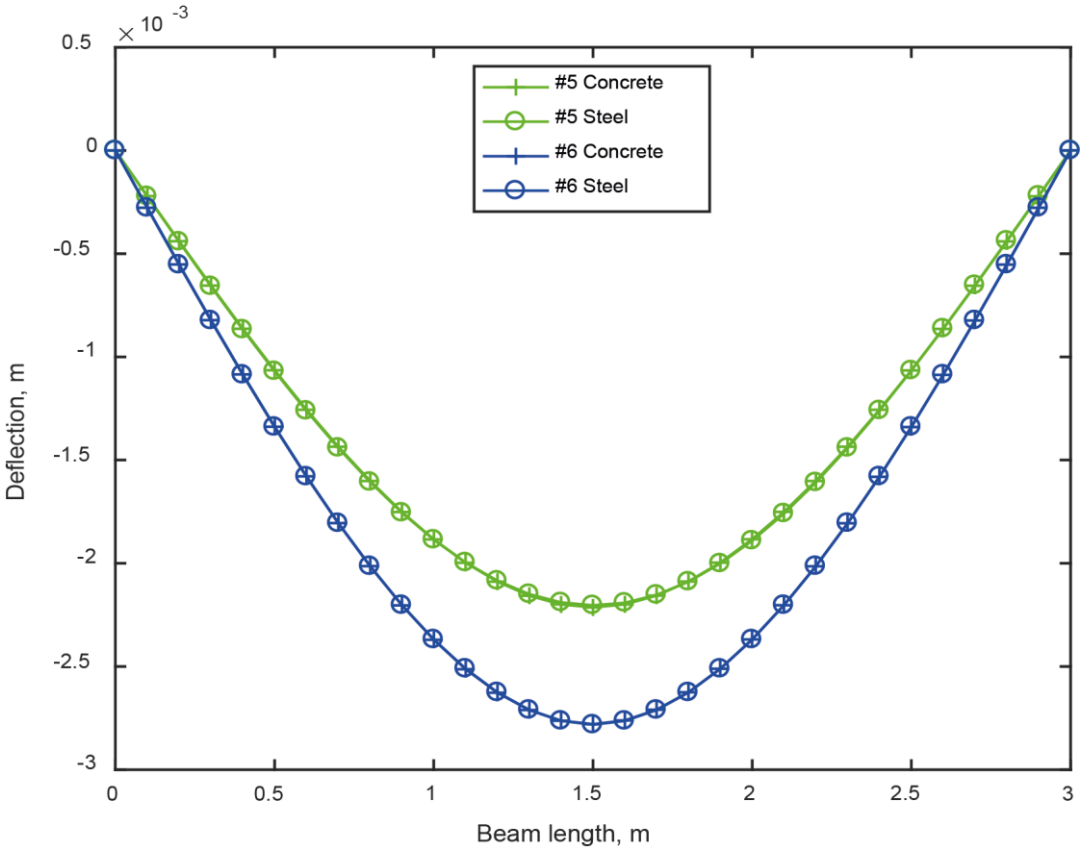

Figure 42. Deflections of beams #5 and #6

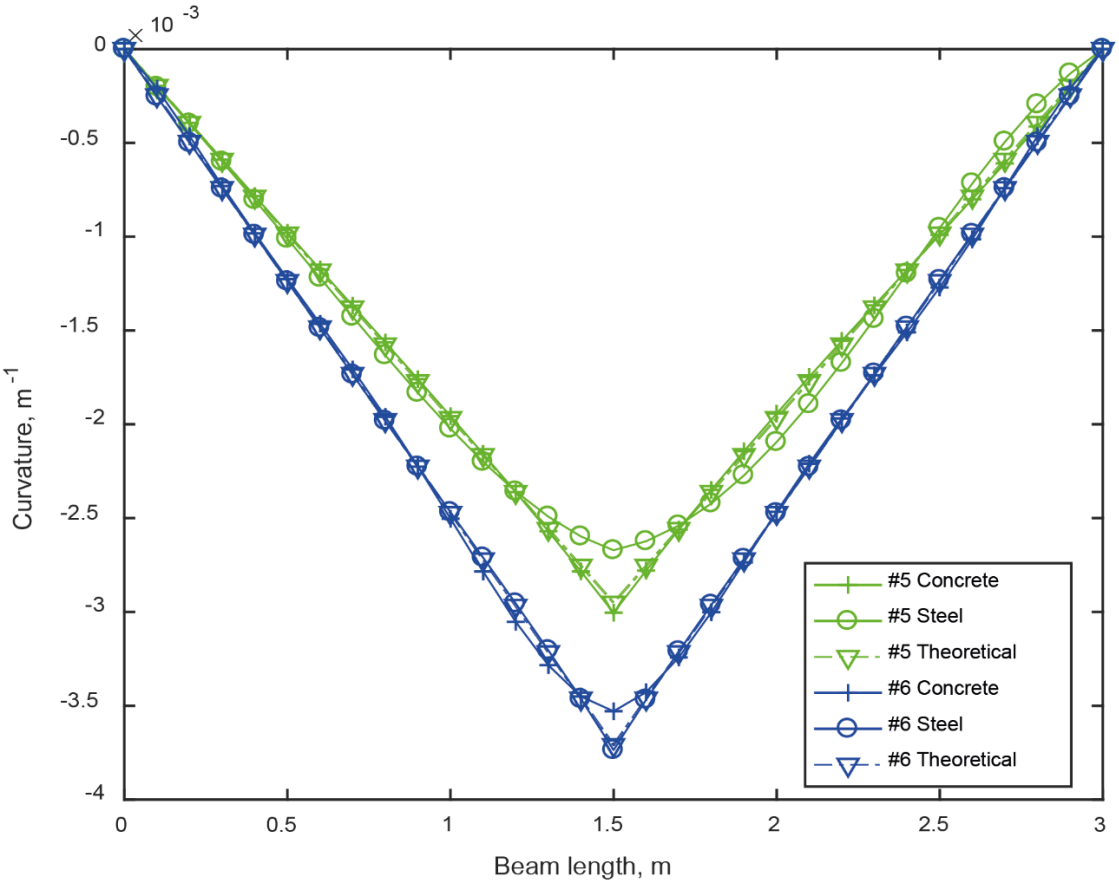

Figure 43. Curvatures of beams #5 and #6

b) 0.5 m thickness - # R, # 7 and # 8

Deflections are shown in Fig. 44. Even though the three beams have the same total thickness, they present different deflections due to the different values of stiffness's that each one of them has. The reference beam presents the lower stiffness, followed by the beam #7 and finally the beam #8. Again, as in for the cases of total thickness of value 0.4 m, the model is able to represent accurately the different effect of different thicknesses.

Curvatures are plotted in Fig. 45. It can be noticed that, for both beams, at mid-span, calculated curvatures from the model does not coincide with the theoretical one, as before. In the beam #7, it is the concrete curvature which has a little oscillation. On the other hand, in the beam #8, it is the concrete curvature which has this behavior.

Regarding curvatures, is for the element of the beam of less thickness, in which is related curvature presents this oscillation.

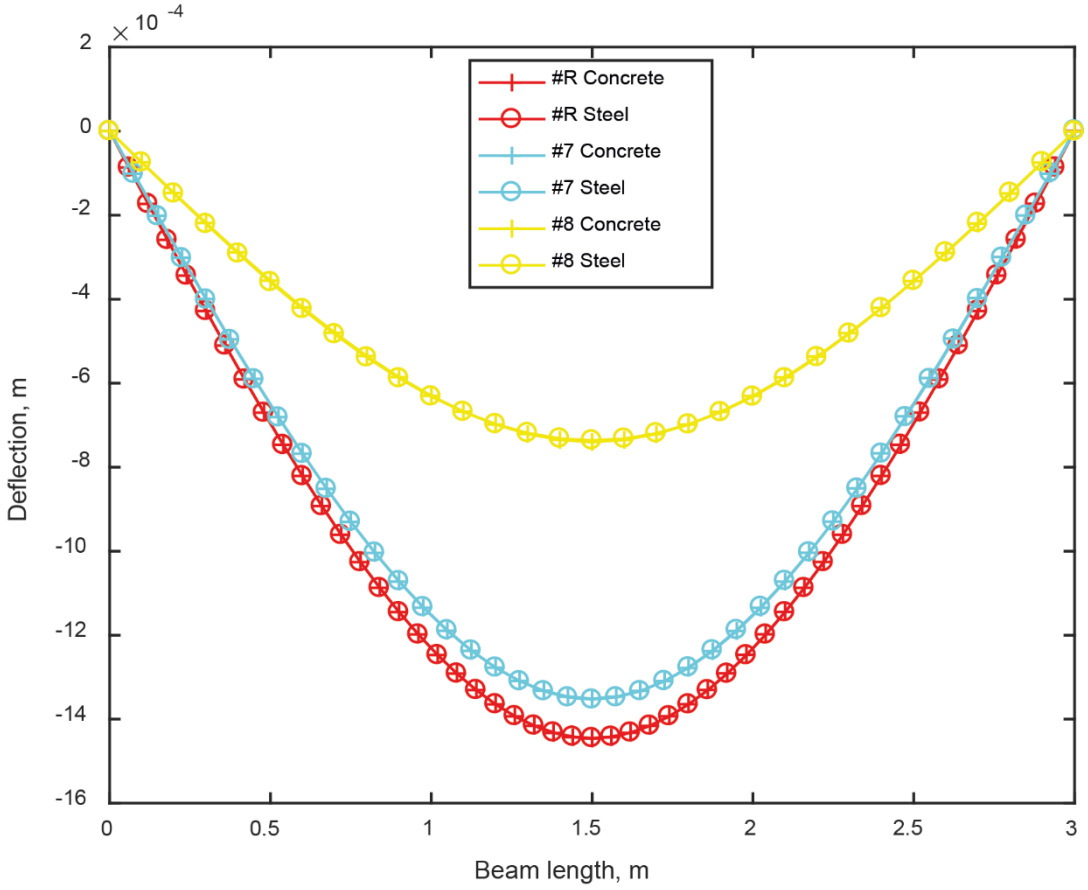

Figure 44. Deflections of beams #R, #7 and #8

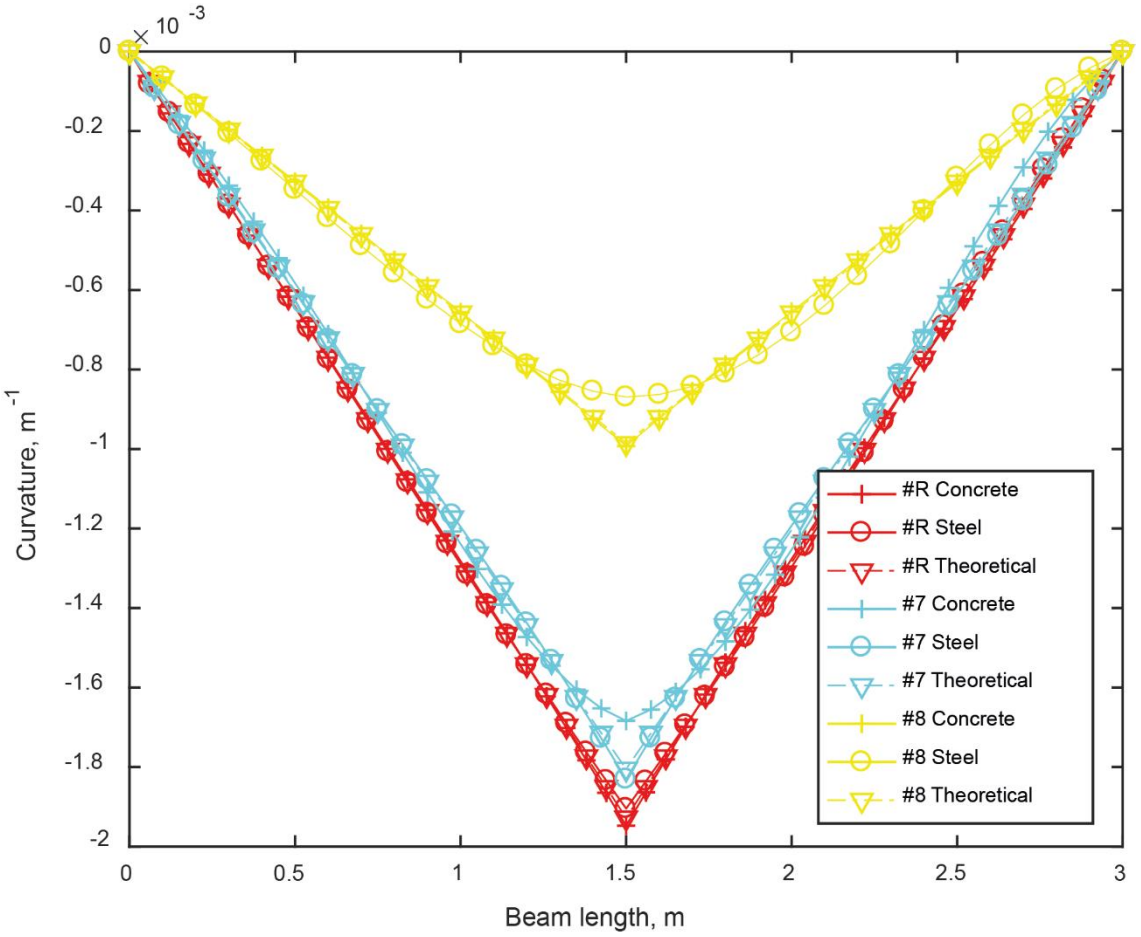

Figure 45. Curvatures of beams #R, #7 and #8

6. CONCLUSIONS

6.1 SUMMARY OF THE WORK

The purpose of the present study was to develop a model for the analysis of steel and concrete composite beams without shear interaction that considers the adjustment of the horizontal displacement of the interface of contact by means of the theory of strength of materials, and compare it to previous models established in former researches.

In this sense, a numerical model was developed by using the programming software *Matlab*. This programming tool allowed to solve the non-linear system of equations defining the problem under study.

The model is validated on a simply supported beam, a static determinate structure, in order to ease some structural aspects. Besides, this case was also proved by previous models and it facilitated the work of comparison.

The principal load case used to define the model was a punctual load at mid-span. Plus, the model was also tested for a distributed load.

Finally, it was conducted a parametrical study, in which different thickness/relations of the beam were analyzed, in order to see the capacity of the model to calculate various situations, as the procedure of the model is highly link to the case under study.

In conclusion, the developed model which considered the adjustment of the horizontal displacement regarding the slip in the interface of contact was created and the effect of this assumption was evaluated.

6.2 CONCLUSIONS

After developing the model and presenting the results, some conclusions may be extracted by gathering all knowledge obtained.

The main conclusion, regarding the motivation for the proposed thesis, is that the new assumption for the horizontal displacement, which defined a new system of equations defining the problem, is proved to be no relevant for modelling composite beams with partial interaction. Curvatures of concrete and steel are tested to be practically equal (. Thus, they can be considered as such, as it has been considered in the literature until now. The fact that the it has been checked for a composite beam without shear connection, it ensures it will be fulfilled for any composite beam with any grade of partial interaction, as when there is not shear connection the slip is the highest possible because it is not physically restricted.

Apart from the stated above, some other conclusions may be presented as supporting feature:

- For the applied examples, the tolerance on the model can be accepted as the errors are due to numerical process and can be neglected.
- Model is able to analyze a simply supported beam, but it may not be applicable to a number of common structures (such as statically indeterminate and tapered beams).
- The model, based on the updated equation regarding the horizontal displacement at the interface, is able to analyze simply supported composite beams with any type of load applied.
- Regarding analyzing the case for different stiffness's, the model represents accurately deflections but some oscillations appear in the curvatures, usually on curvature for the element of less thickness.
- The larger the beam span, the fewer number of elements with which the model is able to get a solution.

BIBLIOGRAPHY

- Dall'Asta, A. and Zona, A. (2002). Non-linear analysis of composite beams by a displacement approach, Comput. Struct. 80 (27–30) 2217–2228.
- EN 1994-1-1 (1994). Eurocode 4: Design of composite steel and concrete structures - Part 1-1: General rules and rules for buildings, European Committee of Normalization.
- EN 1994-2 (1994). Eurocode 4: Design of composite steel and concrete structures - Part 2: General rules and rules for bridges, European Committee of Normalization.
- Gattesco, N. (1999). "Analytical modeling of nonlinear behavior of composite beams with deformable connection". In: Journal of Constructional Steel Research 52.2, pp. 195–218.
- Johnson, R. P. (2004). Composite Structures of Steel and Concrete. Ed. by R. Johnson. Vol. 19. 4.Oxford, UK: Blackwell Publishing Ltd, p. 338.
- Li, G.-Q. and Li, J.-J. (2007). Advanced Analysis and Design of Steel Frames. Chichester, UK: John Wiley & Sons, Ltd, p. 392.
- Martínez, J. and Ortiz, J. (1975). Composite construction, Construcción Mixta, Editorial Rueda,1975. (In Spanish).
- Newmark, N.M., Siess, C.P. and Viest, I.M. (1951). Tests and analysis of composite beams with incomplete interaction, Proc. Soc. Exp. Stress Anal. 9 (1) 7592.
- Proco, G., Spadea, G. and Zinno, R. (1994). Finite element analysis and parametric study of steel–concrete composite beams, Cem. Concr. Compos. 16 261–272.
- Queiroz, F.D., Vellasco, P.C.G.S. and Nethercot, D.A. (2007). Finite element modeling of composite beams with full and partial shear connection, J. Constr. Steel Res. 63 (4) 505–521.
- Queiroz, F.D., Queiroz, G. and Nethercot, D.A. (2009). Two-dimensional FE model for evaluation of composite beams, I: formulation and validation, J. Constr. Steel Res. 65 1055–1062.
- Queiroz, F.D., Queiroz, G. and Nethercot, D.A. (2009). Two-dimensional FE model for evaluation of composite beams, II: parametric study, J. Constr. Steel Res. 65 1063–1074.

- Turmo, J. and Mirambell, E. Calculation model for composite structures with imperfect interaction. Modelo de cálculo para estructuras mixtas con interacción imperfecta, II International conference of ACHE (Asociación Científico Técnica del Hormigón Estructural), 11–14 November, Madrid, 2002 (In Spanish).
- Turmo, J., Lozano-Galant, J.A., Mirambell, E. and Xu, D. (2015). Modeling composite beams with partial interaction, J. Constr. Steel Res. 114 380–393.
- Vasdravellis, G., Uy, B., Tan, E. L., and Kirkland, B. (2012). "Behaviour and design of composite beams subjected to negative bending and compression". In: Journal of Constructional Steel Research 79, pp. 34–47.

APPENDICES

Appendix 1 – Main Script for a punctual load

```
clc
clear all
close all

%----------------------------- MODEL-------------------------%
%% INTRODUCTION
%% Definition of the physical parameters

% Length of the composite beam
L=3;

% Young's modulus of concrete, in kN/m2
E_c= 3.2E7;

% Young's modulus of steel, in kN/m2
E_s= 2.1E8;

% Moment of intertia of concrete, in m4
I_c= 6.67E-4;

% Moment of intertia of steel, in m4
I_s= 8.36E-5;

% H_c is the concrete slab thickness, in m
H_c= 0.2;

% H_s is the steel beam thickness, in m
H_s= 0.3;

% F is the punctual force applied on the composite beam, in kN
F=100;

% Obtaining, from physical parameters, values needed for the model
EI_c=E_c*I_c;
EI_s=E_s*I_s;

% h_c is the distance from the concrete centroid to the interface,
% half of the thickness as it is found in the middle, in M
h_c=H_c/2;

% h_s is the distance from the steel centroid to the interface,
% half of the thickness as it is found in the middle, in m
```

```
h_s=H_s/2;

%% Definition of the numerical parameters

% Number of elements in which the beam is divided
n_elem=50;

% Tolerance
tol=1e-6;

% Scaling factor
D=1/EI_s;

%%  Definition of the vector of cross sections at steel coordinates

% Number of cross sections
n_points=n_elem + 1;

% Distance between cross sections
deltax_s=L/n_elem;

% x_s is the vector containing the steel centroid coordinates for each
% cross section
x_s = [0:deltax_s:L];

%% Calculation of the bending moment due to external load at cross
% sections

% In order to get the bending moment law if the punctual load is at
% mid-span
a=L/2;
i_division= 0:deltax_s:L;
[M]= ssb_plmd_i(i_division,L,F,a);
M=M(2:n_points-1);


%% Vector of unknowns X

% x_c is the vector containing the concrete centroid coordinates for
% each cross section. As first guess, it is considered equal to x_s
x_c=x_s;

% k_c is the vector containing the curvature of concrete at each
% centroid concrete coordinate
k_c=zeros(1,n_points-2);

% k_s is the vector containing the curvature of steel at each centroid
% steel coordinate
k_s=zeros(1,n_points-2);

% theta_c0 is the rotation of concrete at the left support
theta_c0=-(1*F*L*L)/(16*(EI_c+EI_s));

% theta_s0 is the rotation of steel at the left support
theta_s0=-(1*F*L*L)/(16*(EI_c+EI_s));

% Vector X gathers up all unknowns and variables for the optimmization
% problem
```

```
X=[x_c k_c k_s theta_c0 theta_s0];


%% OPTIMIZATION
%% Initial parameters
% For the optmization, there have to be defined some parameters.

% Vector X does not have lower and upper bounds

% Application of non-linear equality defined in the function rest_c

% Initial values are defined, from which optmization will begin.
%Value from traditional theory are chosen

alpha=EI_c/(EI_c+EI_s);
initial_values = [x_s alpha*M/(EI_c+EI_s) (1-alpha)*M/(EI_c+EI_s)...
    theta_c0 theta_s0];


%Finally, it is defined the algorithm used to solve the optimization
options = optimoptions ('fmincon','Algorithm','interior-point');

%% Procedure of optimization and obtaining of X

% Vector solution X is obtained by optimization, which minimizes the
% system of non-linear equations, defined inf function syst_eq
[X,f,exit,output] = fmincon(@(X)...
    syst_eq(X,x_s,h_c,h_s,EI_c,EI_s,M,n_points,D),initial_values,...
    [],[],[],[],[],[],@(X) rest_c(X,h_c,h_s,n_points),options);

% Readjustment of the vector X, considering the values that are known
% for structural reasons
x_c = X(1:n_points);
k_c = X(n_points+1:2*n_points-2);
k_s = X(2*n_points-1:3*n_points-4);
theta_c0=X(3*n_points -3);
theta_s0= X(3*n_points -2);
X = [x_c 0 k_c 0 0 k_s 0 theta_c0 theta_s0];

%% Deflections and rotations
% It is possible to take a first look at the obtained solution
[u_c] = deflection_c(X(3*n_points +1),X(1:n_points),...
    X(n_points+1:2*n_points),n_points);
[u_s] = deflection_s(X(3*n_points +2),x_s,...
    X(2*n_points+1:3*n_points),n_points);


theta_c = calc_theta_c(X(3*n_points +1),X(1:n_points),...
    X(n_points+1:2*n_points),n_points);
theta_s = calc_theta_s(X(3*n_points +2),x_s,...
    X(2*n_points+1:3*n_points),n_points);

% Deflections at right support are not satisfied. Loof for a better
% result

%% Satisfying null deflection condition at the right-hand side support
% Knowing that deflection at the edge of the beam must be 0, this
% contition is imposed, and solved by using the function "while"
```

```
% Condition for which deflection of concrete is 0 at right support
cond_1 = abs(u_c(n_points))<tol;

% Condition for which deflection of steel is 0 at right support
cond_2 = abs(u_s(n_points))<tol;

% Vector of initial rotations of concrete, used in the while loop
theta_c0_vector(1)=theta_c0;

% Vector of initial rotations of steel, used in the while loop
theta_s0_vector(1)=theta_s0;

% Vector of deflections of concrete at the right support, used in the
% while loop
u_c_vector(1)=u_c(end);

% Vector of deflections of steel at the right support, used in the
% while loop
u_s_vector(1)=u_s(end);

% i_count is the number of steps to satisfy cond_1 and cond_2 with the
% established tolerance
i_count=1;

% While loop
while not(and(cond_1,cond_2))

    i_count
    theta_c0_vector(i_count+1)=theta_c0_vector(i_count)-...
        u_c_vector(i_count)/L;
    theta_s0_vector(i_count+1)=theta_s0_vector(i_count)-...
        u_s_vector(i_count)/L;

    initial_values = [x_s alpha*M/(EI_c+EI_s) (1-
alpha)*M/(EI_c+EI_s)...
        theta_c0_vector(i_count+1) theta_s0_vector(i_count+1)];

    [X,f,exit,output] = fmincon(@(X)
syst_eq(X,x_s,h_c,h_s,EI_c,EI_s,...
        M,n_points,D),initial_values,[],[],[],[],[],[],...
        @(X) rest_c(X,h_c,h_s,n_points),options);

    x_c = X(1:n_points);
    k_c = X(n_points+1:2*n_points-2);
    k_s = X(2*n_points-1:3*n_points-4);
    theta_c0=X(3*n_points -3);
    theta_s0= X(3*n_points -2);
    X = [x_c 0 k_c 0 0 k_s 0 theta_c0 theta_s0];

    [u_c] = deflection_c(X(3*n_points +1),X(1:n_points),...
        X(n_points+1:2*n_points),n_points);
    [u_s] = deflection_s(X(3*n_points +2),x_s,...
        X(2*n_points+1:3*n_points),n_points);
    u_c_vector(i_count+1)=u_c(end);
    u_s_vector(i_count+1)=u_s(end);

    cond_1 = abs(u_c(n_points))<tol;
    cond_2 = abs(u_s(n_points))<tol;
```

```
    i_count=i_count+1;
end

%% RESULTS
%% Concrete centroid coordinates, curvature of concrete and steel
x_c = X(1:n_points);
k_c = X(n_points+1:2*n_points);
k_s = X(2*n_points+1:3*n_points);

[M]= ssb_plmd_i(i_division,L,F,a);

%% Deflections and rotations

[u_c] = deflection_c(X(3*n_points +1),X(1:n_points),...
    X(n_points+1:2*n_points),n_points);
[u_s] = deflection_s(X(3*n_points +2),x_s,...
    X(2*n_points+1:3*n_points),n_points);


theta_c = calc_theta_c(X(3*n_points +1),X(1:n_points)...
    ,X(n_points+1:2*n_points),n_points);
theta_s = calc_theta_s(X(3*n_points +2),x_s,...
    X(2*n_points+1:3*n_points),n_points);

%% Plots and graphs

% Deflections of concrete and steel
figure(1);
plot(x_c,u_c,'r+-');
hold on
plot(x_s,u_s,'go-');
xlabel('Beam length, m');
ylabel('Deflection, m');
legend({'Concrete','Steel'},'location','best')

% Rotations of concrete and steel
figure(2);
plot(x_c,theta_c,'r+-');
hold on
plot(x_s,theta_s,'go-');
xlabel('Beam length, m');
ylabel('Rotation, rad');
legend({'Concrete','Steel'},'location','best')

% Residues of equations
[Y_sum,Y] = syst_eq(X,x_s,h_c,h_s,EI_c,EI_s,M,n_points,D);
figure(3);
semilogy(abs(Y(1:3:end-2)),'r-');
hold on
semilogy(abs(Y(2:3:end-2)),'g-');
semilogy(abs(Y(3:3:end-2)),'b-');
legend({'1st equation','2nd equation','3rd equation'},...
    'location','best')

% Curvatures of concrete and steel
figure(4);
plot(x_c,-k_c,'r+-');
hold on
plot(x_s,-k_s,'go-');
```

```
plot(x_s,-M/(EI_s+EI_c),'bv-.')
xlabel('Beam length, m');
ylabel('Curvature, m^{-1}');
legend({'Concrete','Steel','Theoretical'},'location','best')
```

Appendix 2 – Main script for a distributed load

```
clc
clear all
close all

%----------------------------- MODEL--------------------------%
%% INTRODUCTION
%% Definition of the physical parameters

% Length of the composite beam
L=3;

% Young's modulus of concrete, in kN/m2
E_c= 3.2E7;

% Young's modulus of steel, in kN/m2
E_s= 2.1E8;

% Moment of intertia of concrete, in m4
I_c= 6.67E-4;

% Moment of intertia of steel, in m4
I_s= 8.36E-5;

% H_c is the concrete slab thickness, in m
H_c= 0.2;

% H_s is the steel beam thickness, in m
H_s= 0.3;

% q is the distributed load applied on the composite beam, in kN/m
q=100;

% Obtaining, from physical parameters, values needed for the model
EI_c=E_c*I_c;
EI_s=E_s*I_s;

% h_c is the distance from the concrete centroid to the interface,
% half of the thickness as it is found in the middle, in M
h_c=H_c/2;

% h_s is the distance from the steel centroid to the interface,
% half of the thickness as it is found in the middle, in m
h_s=H_s/2;
%% Definition of the numerical parameters

% Number of elements in which the beam is divided
n_elem=40;

% Tolerance
```

```
tol=1e-6;

% Scaling factor
D=1/EI_s;

%%  Definition of the vector of cross sections at steel coordinates

% Number of cross sections
n_points=n_elem + 1;

% Distance between cross sections
deltax_s=L/n_elem;

% x_s is the vector containing the steel centroid coordinates for each
% cross section
x_s = [0:deltax_s:L];

%% Calculation of the bending moment due to external load at cross
% sections

i_division= 0:deltax_s:L;
[M]= ssb_dl_i(i_division,L,q);
M=M(2:n_points-1);

%% Vector of unknowns X

% x_c is the vector containing the concrete centroid coordinates for
% each cross section. As first guess, it is considered equal to x_s
x_c=x_s;

% k_c is the vector containing the curvature of concrete at each
% centroid concrete coordinate
k_c=zeros(1,n_points-2);

% k_s is the vector containing the curvature of steel at each centroid
% steel coordinate
k_s=zeros(1,n_points-2);

% theta_c0 is the rotation of concrete at the left support
theta_c0=-(q*L*L*L)/(24*(EI_c+EI_s));

% theta_s0 is the rotation of steel at the left support
theta_s0=-(q*L*L*L)/(24*(EI_c+EI_s));

% Vector X gathers up all unknowns and variables for the optimmization
% problem
X=[x_c k_c k_s theta_c0 theta_s0];

%% OPTIMIZATION
%% Initial parameters
% For the optmization, there have to be defined some parameters.

% Vector X does not have lower and upper bounds

% Application of non-linear equality defined in the function rest_c

% Initial values are defined, from which optmization will begin.
%Value from traditional theory are chosen
```

```
alpha=EI_c/(EI_c+EI_s);
initial_values = [x_s alpha*M/(EI_c+EI_s) (1-alpha)*M/(EI_c+EI_s)...
    theta_c0 theta_s0];


%Finally, it is defined the algorithm used to solve the optimization
options = optimoptions ('fmincon','Algorithm','interior-point');

%% Procedure of optimization and obtaining of X

% Vector solution X is obtained by optimization, which minimizes the
% system of non-linear equations, defined inf function syst_eq
[X,f,exit,output] = fmincon(@(X)...
    syst_eq(X,x_s,h_c,h_s,EI_c,EI_s,M,n_points,D),initial_values,...
    [],[],[],[],[],[],@(X) rest_c(X,h_c,h_s,n_points),options);

% Readjustment of the vector X, considering the values that are known
% for structural reasons
x_c = X(1:n_points);
k_c = X(n_points+1:2*n_points-2);
k_s = X(2*n_points-1:3*n_points-4);
theta_c0=X(3*n_points -3);
theta_s0= X(3*n_points -2);
X = [x_c 0 k_c 0 0 k_s 0 theta_c0 theta_s0];

%% Deflections and rotations
% It is possible to take a first look at the obtained solution
[u_c] = deflection_c(X(3*n_points +1),X(1:n_points),...
    X(n_points+1:2*n_points),n_points);
[u_s] = deflection_s(X(3*n_points +2),x_s,...
    X(2*n_points+1:3*n_points),n_points);


theta_c = calc_theta_c(X(3*n_points +1),X(1:n_points),...
    X(n_points+1:2*n_points),n_points);
theta_s = calc_theta_s(X(3*n_points +2),x_s,...
    X(2*n_points+1:3*n_points),n_points);

% Deflections at right support are not satisfied. Loof for a better
% result

%% Satisfying null deflection condition at the right-hand side support
% Knowing that deflection at the edge of the beam must be 0, this
% contition is imposed, and solved by using the function "while"

% Condition for which deflection of concrete is 0 at right support
cond_1 = abs(u_c(n_points))<tol;

% Condition for which deflection of steel is 0 at right support
cond_2 = abs(u_s(n_points))<tol;

% Vector of initial rotations of concrete, used in the while loop
theta_c0_vector(1)=theta_c0;

% Vector of initial rotations of steel, used in the while loop
theta_s0_vector(1)=theta_s0;
```

```
% Vector of deflections of concrete at the right support, used in the
% while loop
u_c_vector(1)=u_c(end);

% Vector of deflections of steel at the right support, used in the
% while loop
u_s_vector(1)=u_s(end);

% i_count is the number of steps to satisfy cond_1 and cond_2 with the
% established tolerance
i_count=1;

% While loop
while not(and(cond_1,cond_2))

    i_count
    theta_c0_vector(i_count+1)=theta_c0_vector(i_count)-...
        u_c_vector(i_count)/L;
    theta_s0_vector(i_count+1)=theta_s0_vector(i_count)-...
        u_s_vector(i_count)/L;

    initial_values = [x_s alpha*M/(EI_c+EI_s) (1-
alpha)*M/(EI_c+EI_s)...
        theta_c0_vector(i_count+1) theta_s0_vector(i_count+1)];

    [X,f,exit,output] = fmincon(@(X)
syst_eq(X,x_s,h_c,h_s,EI_c,EI_s,...
        M,n_points,D),initial_values,[],[],[],[],[],[],...
        @(X) rest_c(X,h_c,h_s,n_points),options);

    x_c = X(1:n_points);
    k_c = X(n_points+1:2*n_points-2);
    k_s = X(2*n_points-1:3*n_points-4);
    theta_c0=X(3*n_points -3);
    theta_s0= X(3*n_points -2);
    X = [x_c 0 k_c 0 0 k_s 0 theta_c0 theta_s0];

    [u_c] = deflection_c(X(3*n_points +1),X(1:n_points),...
        X(n_points+1:2*n_points),n_points);
    [u_s] = deflection_s(X(3*n_points +2),x_s,...
        X(2*n_points+1:3*n_points),n_points);
    u_c_vector(i_count+1)=u_c(end);
    u_s_vector(i_count+1)=u_s(end);

    cond_1 = abs(u_c(n_points))<tol;
    cond_2 = abs(u_s(n_points))<tol;
    i_count=i_count+1;
end

%% RESULTS
%% Concrete centroid coordinates, curvature of concrete and steel
x_c = X(1:n_points);
k_c = X(n_points+1:2*n_points);
k_s = X(2*n_points+1:3*n_points);

[M]= ssb_dl_i(i_division,L,q);

%% Deflections and rotations
```

```
[u_c] = deflection_c(X(3*n_points +1),X(1:n_points),...
    X(n_points+1:2*n_points),n_points);
[u_s] = deflection_s(X(3*n_points +2),x_s,...
    X(2*n_points+1:3*n_points),n_points);


theta_c = calc_theta_c(X(3*n_points +1),X(1:n_points)...
    ,X(n_points+1:2*n_points),n_points);
theta_s = calc_theta_s(X(3*n_points +2),x_s,...
    X(2*n_points+1:3*n_points),n_points);

%% Plots and graphs

% Deflections of concrete and steel
figure(1);
plot(x_c,u_c,'r+-');
hold on
plot(x_s,u_s,'go-');
xlabel('Beam length, m');
ylabel('Deflection, m');
legend({'Concrete','Steel'},'location','best')

% Rotations of concrete and steel
figure(2);
plot(x_c,theta_c,'r+-');
hold on
plot(x_s,theta_s,'go-');
xlabel('Beam length, m');
ylabel('Rotation, rad');
legend({'Concrete','Steel'},'location','best')

% Residues of equations
[Y_sum,Y] = syst_eq(X,x_s,h_c,h_s,EI_c,EI_s,M,n_points,D);
figure(3);
semilogy(abs(Y(1:3:end-2)),'r-');
hold on
semilogy(abs(Y(2:3:end-2)),'g-');
semilogy(abs(Y(3:3:end-2)),'b-');
legend({'1st equation','2nd equation','3rd equation'},...
    'location','best')

% Curvatures of concrete and steel
figure(4);
plot(x_c,-k_c,'r+-');
hold on
plot(x_s,-k_s,'go-');
plot(x_s,-M/(EI_s+EI_c),'bv-.')
xlabel('Beam length, m');
ylabel('Curvature, m^{-1}');
legend({'Concrete','Steel','Theoretical'},'location','best')
```

Appendix 3 – Bending moment under punctual load. Function ssb_plmd_i

```
% Function to get the bending moment at each cross section
function [M] = ssb_plmd_i (i,L,F,a)
```

```
M=((i>=0)&(i<=a)).*(F*(L-a)*i/L)+ ((i>a)&(i<=L)).*((F*a*(L-i))/L);
end
```

Appendix 4 - Bending moment under distributed load. Function ssbd_dl_i

```
% Function to get the bending moment at each cross section
function [M] = ssb_dl_i (i,L,F)
M=F*i.*(L-i)/2;
end
```

Appendix 5 – System of equations. Function syst_eq

```
% System of equations to be minimized
function  [Y_sum,Y] = syst_eq(X,Xs,hc,hs,EIc,EIs,M,n_points,D)
Xc=X(1:n_points);
Kc=X(n_points+1:2*n_points-2);
Kc=[0 Kc 0];
Ks=X(2*n_points-1:3*n_points-4);
Ks=[0 Ks 0];
theta_c0=X(3*n_points -3);
theta_s0=X(3*n_points -2);

X=[Xc Kc Ks theta_c0 theta_s0];
M=[0 M 0];
[theta_c]= calc_theta_c(theta_c0,Xc,Kc,n_points);
[theta_s]= calc_theta_s(theta_s0,Xs,Ks,n_points);
[u_c] = deflection_c(theta_c0,Xc,Kc,n_points);
[u_s] = deflection_s(theta_s0,Xs,Ks,n_points);


for i = 2:n_points
% 1st equation
Y(3*i-2)= (u_c(i-1)+(Xc(i)-Xc(i-1))*theta_c(i-1)+ (Kc(i)+2*Kc(i-
1))/...
    6*(Xc(i)-Xc(i-1))^2 -u_s(i-1) -(Xs(i)-Xs(i-1))*theta_s(i-1)- ...
    (Ks(i)+2*Ks(i-1))/6*(Xs(i)-Xs(i-1))^2);

% 2nd equation
Y(3*i-1)=(Xc(i) + hc*theta_c(i)- Xs(i) + hs*theta_s(i));

% 3rd equation
Y(3*i)= (Ks(i)*EIs +(Kc(i-1)+(Kc(i)-Kc(i-1))/(Xc(i)-Xc(i-1))*...
    (Xs(i)-Xc(i-1)))*EIc - M(i))*D;

end
%Deflection of steel at right hand side, which must be zero
Y(3*n_points+1)= u_c(n_points);

%Deflection of steel at right hand side, which must be zero
Y(3*n_points+2)= u_s(n_points);

Y_sum=sum(Y.^2);
end
```

Appendix 6 – Restriction at 1st cross section. Function rest_c

```
% Function called in the optimization for the restriction on the 1st
% cross section
function [c,ceq] = rest_c(X,hc,hs,n_points)
Xc=X(1:n_points);
Kc=X(n_points+1:2*n_points-2);
Kc=[0 Kc 0];
Ks=X(2*n_points-1:3*n_points-4);
Ks=[0 Ks 0];
theta_c0=X(3*n_points -3);
theta_s0=X(3*n_points -2);

X=[Xc Kc Ks theta_c0 theta_s0];
c=[];
ceq= X(1) + hc*X(3*n_points+1) + hs*X(3*n_points+2);
end
```

Appendix 7 – Rotation of concrete element. Function calc_theta_c

```
%Function to obtain the vector of rotations at the concrete beam
function theta_c = calc_theta_c(theta_c0,xc,kc,n_points)
theta_c(1)=theta_c0;
for i=2:n_points
    theta_c(i)=theta_c(i-1) + ((kc(i)+kc(i-1))*(xc(i)-xc(i-1))/2);
end
end
```

Appendix 8 – Rotation of steel element. Function calc_theta_s

```
%Function to obtain the vector of rotations at the steel beam
function theta_s = calc_theta_s(theta_s0,xs,ks,n_points)
theta_s(1)=theta_s0;
for i=2:n_points
    theta_s(i)=theta_s(i-1) + ((ks(i)+ks(i-1))*(xs(i)-xs(i-1))/2);
end
end
```

Appendix 9 – Deflection of concrete element. Function deflection_c

```
%Function to obtain the vector of deflections at the concrete beam
function u_c = deflection_c(theta_c0,xc,kc,n_points)
u_c(1)=0;

[theta_c]= calc_theta_c(theta_c0,xc,kc,n_points);
for i=2:n_points
    u_c(i)=u_c(i-1) + (xc(i)-xc(i-1))*theta_c(i-1) + (kc(i)+2*kc(i-
1))...
        /6*(xc(i)-xc(i-1))^2;
end
end
```

Appendix 10 – Deflection of steel element. Function deflection_s

```
%Function to obtain the vector of deflections at the steel beam
function u_s = deflection_s(theta_s0,xs,ks,n_points)
u_s(1)=0;

[theta_s]= calc_theta_s(theta_s0,xs,ks,n_points);
for i=2:n_points
    u_s(i)=u_s(i-1) + (xs(i)-xs(i-1))*theta_s(i-1) + (ks(i)+2*ks(i-
1))...
        /6*(xs(i)-xs(i-1))^2;
end
end
```